The feasibility of patient-specific circulating tumor DNA monitoring throughout multi-modality therapy for locally advanced esophageal and rectal cancer: A potential biomarker for early detection of subclinical disease

Short title: **CtDNA monitoring throughout multimodal therapy**

Christopher Boniface, BA[1,2], Christopher Deig, MD[3], Carol Halsey, BS[4], Taylor Kelley, BS[4], Michael B. Heskett, BS[4], Charles R. Thomas Jr., MD[3], Paul T. Spellman, PhD[1,4], and Nima Nabavizadeh, MD[3,5]

[1]Cancer Early Detection Advanced Research (CEDAR) Center, Knight Cancer Institute, Oregon Health & Science University (OHSU), 2720 SW Moody Ave. Portland, OR 97201
[2]Department of Biomedical Engineering, Oregon Health & Science University (OHSU) School of Medicine, 3181 SW Sam Jackson Park Rd, Portland, OR 97239
[3]Department of Radiation Medicine, Oregon Health & Science University (OHSU), 3181 SW Sam Jackson Park Rd, KPV4, Portland, OR 97239
[4]Department of Molecular and Medical Genetics, Oregon Health & Science University (OHSU) School of Medicine, 3181 SW Sam Jackson Park Rd, Portland, OR 97239
[5] Corresponding author – nabaviza@ohsu.edu; 503-494-8756

Author Contributions

CB authored this report, produced all figures, carried out all laboratory work for data generation, and conducted all data analysis. CD edited this report and aggregated de-identified patient clinical information and imaging. NN, CH and TK identified and consented potential study candidates. CH and TK procured patient biological samples. MBH assisted in statistical analysis and provided code. CRT, PTS, and NN conceived this project, edited and gave final approval for this manuscript. PTS and NN procured funding.

Data availability statement

The data used for analysis in this report consisted of de-identified patient clinical information and next-generation sequencing data using both custom capture and whole-exome capture library preparations. Patient clinical data are presented in the report and sequencing data (BAM files) are available on the Sequence Read Archive website (www.ncbi.nlm.nih.gov/sra) under the BioProject accession number PRJNA637431 (https://www.ncbi.nlm.nih.gov/sra/PRJNA637431).

Funding Statement

NN received funding for this project through an American Society for Clinical Oncology Young Investigator Award (https://www.asco.org/) and a Radiological Society of North America Seed Grant (https://www.rsna.org/). The funders had no role in study design, data collection and analysis, decision to publish, or preparation of the manuscript.

Ethics Statement

In this feasibility study, human specimens and data (including blood, tumor tissue, and clinical information) were prospectively acquired from participants with locally-advanced esophageal (n=3) or rectal cancer (n=2) undergoing definitive multimodal therapy after their informed written consent (Oregon Health & Science University, IRB# 10163).

Conflicts of Interest Statement

All authors listed are free of any conflicts of interest related to this work.

Keywords

liquid biopsy; ctDNA; cell free DNA; non-operative management; neoadjuvant therapy

Abstract

As non-operative management (NOM) of esophageal and rectal cancer is becoming more prevalent, blood-biomarkers such as circulating tumor DNA (ctDNA) may provide clinical information in addition to endoscopy and imaging to aid in treatment decisions following chemotherapy and radiation therapy. In this feasibility study, we prospectively collected plasma samples from locally advanced esophageal (n=3) and rectal cancer (n=2) patients undergoing multimodal neoadjuvant therapy to assess the feasibility of serial ctDNA monitoring throughout neoadjuvant therapy. Using the DIDA-Seq error-correction method, we serially interrogated plasma cell-free DNA at 28-41 tumor-specific genomic loci throughout therapy and in surveillance with an average limit of detection of 0.016% mutant allele frequency. In both rectal cancer patients, ctDNA levels were persistently elevated following total neoadjuvant therapy with eventual detection of clinical recurrence prior to salvage surgery. Among the esophageal cancer patients, ctDNA levels closely correlated with tumor burden throughout and following neoadjuvant therapy, which was associated with a pathologic complete response in one patient. In this feasibility study, patient and tumor-specific ctDNA levels correlated with clinical outcomes throughout multi-modality therapy suggesting that serial monitoring of patient ctDNA has the potential to serve as a highly sensitive and specific biomarker to risk-stratify esophageal and rectal cancer patients eligible for NOM. Further prospective investigation is warranted.

Introduction

As non-operative management (NOM) of locally-advanced esophageal and rectal cancer following chemotherapy and radiation therapy is more widely adopted [1,2], a sensitive and specific biomarker of sub-clinical tumor burden has the potential of further assisting in the assessment of patients best suited for an upfront non-operative approach or for detecting early sub-clinical

recurrences in patients in need of salvage surgery in the surveillance period [3]. Circulating tumor DNA (ctDNA) has been extensively investigated for its diagnostic and prognostic utility as such a biomarker [4-8]; however, the longitudinal application of ctDNA monitoring throughout multi-modality therapy (systemic therapy, radiotherapy, and/or surgery) has been less extensively studied [4]. Undetectable ctDNA following definitive treatment has been shown to be associated with pathologic complete response (pCR) and improved outcomes, particularly in the neoadjuvant setting for breast cancer [9,10]; however, the feasibility of serial ctDNA measurements in the neoadjuvant setting for rectal and esophageal cancer has not been previously reported.

Our ctDNA monitoring technique, called DIDA-Seq (Dual-Indexed, Degenerate Adaptor-Sequencing), combines unique-molecular indexing (UMI)-based error correction with custom hybridization capture at many genomic loci of somatic variants previously identified by whole-exome sequencing of the patient's tumor tissue. This method allows the detection of ctDNA in the blood with very high accuracy (1 error in 10k-50k observations) and sensitivity (0.005%-0.02% minimum variant allele frequency [11]). This study aims to test the feasibility of using patient and tumor-specific ctDNA monitoring to assess residual disease in five esophageal and rectal cancer patients during and after multimodal neoadjuvant therapy (Fig 1).

Materials and methods

Patient enrollment, tissue processing, and DNA extraction

In this feasibility study, human specimens and data (including blood, tumor tissue, and clinical information) were prospectively acquired from participants with locally-advanced esophageal (n=3) or rectal cancer (n=2) undergoing definitive multimodal therapy after their informed written consent

(Oregon Health & Science University, IRB# 10163). Plasma samples were collected at baseline, throughout therapy and surveillance. Biopsy tissue was collected at diagnosis and recurrence (Fig 1). Blood draws were serially collected and fractionated for cfDNA isolation using the "double spin" method (≤ 40 mL, a range of 6–40 mL, in 5 × 6-mL or 4 × 10-mL, purple-capped EDTA tubes) [8,11]. DNA was extracted from FFPE, plasma and buffy coat using commercially available kits (see below). Within 6 hours of collection, blood plasma was isolated by first spinning whole blood at 1000g for 10 min, separating the top plasma layer into 1-mL aliquots, then spinning those aliquots at 15,000g for 10 min, transferring the supernatant to cryovials, and storing at −80°C. Fixed formalin paraffin-embedded biopsies and tumor-tissue were collected and DNA extraction was carried out using QIAgen FFPE DNA extraction kit (QIAGEN). DNA was extracted from plasma and buffy coat using Macherey-Nagel NucleoSnap and QIAgen Blood and Tissue kits, respectively. All DNA extractions were quantified using the Qubit 3 fluorometric quantification system (ThermoFisher Scientific) and size distribution was checked with a BioAnalyzer 2100 (Agilent Technologies). DNA isolated from FFPE samples and buffy coat were fragmented by sonication to 150bp using a Covaris E220 prior to library preparation (cfDNA was not fragmented prior to ligation).

Whole-Exome Sequencing Library Preparation

Whole-exome sequencing (WES) libraries were prepared from tissue biopsies using 100-500ng of sonicated FFPE of buffy coat DNA and the KAPA Hyper-Prep Kit (KAPA Biosystems) with the Agilent SureSelect XT Target Enrichment System and Human All Exon V5 capture baits (Agilent Technologies). Next generation sequencing was carried out using the Illumina NextSeq 500 platform by our institution's Massively Parallel Sequencing Shared Resource to an average, de-duplicated depth of 329X and 121X for tumor and buffycoat matched-normal libraries, respectively (Supplementary Table 3).

Somatic Mutation Calling and Design of Tumor-Specific Capture Panels

FastQ data files were aligned and processed using BWA MEM (0.7.12, GATK, Broad Institute). Somatic variants were called using aligned BAM files and MuTect (1.1.4, GATK, Broad Institute) between tumor and the patient's matched normal from blood buffy coat [12]. All WES BAM files can be found in the Sequence Read Archive (www.ncbi.nlm.nih.gov/sra) under the BioProject accession number PRJNA637431 [13]. Single nucleotide variant (SNV) calls were filtered out if they were present in the dbSNP database (www.ncbi.nlm.nih.gov/projects/SNP). SNVs were filtered by frequency (requiring >1% variant allele frequency and >3 supporting reads in the tumor, and <2% variant allele frequency in the matched normal) and depth (requiring ≥30X coverage in the tumor and ≥14X coverage in the matched normal) and were further assessed and hand-curated using Oncotator [14] and IGV [15] software. For tumor-specific capture targets, approximately 50 SNVs were chosen for each patient based on inferred clonality, sequence context, and potential functional impact. To address concerns over properly representing cell subpopulations, intronic mutations were included in each panel. Tumor-specific hybrid capture panels were constructed by querying the human reference genome (GRCh37/hg19) for the 120bp surrounding the target loci of interest. The resulting nucleotide sequences were submitted to IDT DNA to generate biotinylated bait oligos using the NGS Discovery Pools tool (https://www.idtdna.com/). Mutation sites and bait oligo sequences are described in Supplementary Table 1.

DIDA-Seq Library Preparation and Sequencing

DIDA-Seq error-correction libraries were prepared similarly to what is previously described and sequenced on Illumina platforms. Briefly, 30-100ng of cell-free DNA was input into the Kapa Biosystems Hyper Prep kit with custom DIDA-Seq adaptors followed by hybridization capture using the IDT xGen Hybridization and Wash Kit using a single, 18 hour capture incubation step instead of the double-

incubation steps previously described [8,11]. Libraries were sequenced on either the Illumina HiSeq 2500, paired-end 100 bp, with dual 14-bp indexing cycles or the Illumina NextSeq 500, paired-end 70 bp with dual 14-bp indexing cycles. All DIDA-Seq BAM files can be found in the Sequence Read Archive (www.ncbi.nlm.nih.gov/sra) under the BioProject accession number PRJNA637431 [13].

Evaluation of Tumor-Specific Capture Panel Performance and CtDNA Prevalence

The error-correction pipeline for analyzing DIDA-Seq data was based on the duplex sequencing pipeline with substantial modification to be compatible with our data [16]. The DIDA-Seq computational pipeline was implemented as previously described [11] and the variant allele frequency (VAF) was determined for each mutation at each time point by dividing the number of mutant error-corrected (*i.e.*, consensus) reads by the total number of consensus reads at that site and multiplying by 100 (note that all VAFs are reported as a percentages in Supplementary Tables). The aggregate VAFs for each time point were calculated by summing the mutant consensus reads at all sites interrogated, dividing that by the total number of consensus reads across all sites and multiplying by 100. Each hybrid capture panel was evaluated using unrelated patient cfDNA samples as negative controls. We sequenced each patient time-point library to a mean, consensus read depth of 5.2kX (range = 159X to 23.4kX) per site-of-interest. We sequenced each negative control library to an average per-site consensus read depth of 43.6kX coverage (range = 3.9kX - 127kX) with an average per-site error rate of 0.0067% or 1 error in 15k site-of-interest observations (range = 1 error in 2.7k to 125k site-of-interest observations) providing an average limit of detection of 0.016% VAF (*i.e.*, the mean of the lowest statistically significant VAF from Patients 2-5, see Supplementary Table 4). When we aggregated negative control site-of-interest consensus read counts for each panel, we calculated an average per-panel error rate of 0.0057%, or 1

error in 17.7k observations with a range of 1 in 12.5k to 22.9k based on the assumption that mutant consensus reads found in the negative control were caused by PCR or sequencer error (see Supplementary Table 2 for panel-specific error rates). We compared the mutation-specific VAF in the patient's plasma at each time-point to the VAF of the same site in the set of pooled negative controls using the Weitzman overlapping coefficient [17] (see "Significance Tests for CtDNA Measurements" below). A p-value was generated for each site, as well as all sites aggregated by tumor-specific panel, using the overlap coefficient between the beta distributions of the sample and the negative control read counts as described below. Any individual site with greater than 0.05% VAF in the negative controls was omitted from evaluation of ctDNA levels in the respective target patient. Data points having a p-value of 0.05 or less were considered significantly different from the negative controls, effectively determining our lower limit of detection given the total sequencing depth at each time point. To correct for differences in cell-free DNA concentration between blood draws, the aggregate VAF was converted into human genome equivalents per ml (hGE/mL) of plasma by the following equation and were plotted longitudinally in Figs 2 through 4:

$$\frac{cfDNA\ concentration\left(\frac{ng}{ml\ plasma}\right)}{0.003\left(\frac{ng}{genome}\right)} * variant\ allele\ frequency$$

$$= Mutant\ genomes\ per\ mL\ plasma\ (or\ hGE/mL\ plasma)$$

Significance Tests for CtDNA Measurements

The significance of ctDNA measurements (*i.e.* mutant consensus reads) at each time point, as compared to the panel's negative control, was determined prior to conversion to human genome equivalents per ml (hGE/mL) plasma and is dependent on the sequencing depth at each site at that time point. A Bayesian approach was used to test the null-hypothesis that the sample VAF and negative control VAF

were generated from the same distribution. This statistical approach was used because we assumed that a higher sample size (*i.e.* deeper sequencing) confers a more accurate parameter estimate (*i.e.,* 100 mutant reads in 100,000 is more accurate than 1 in 100). Therefore, a Beta distribution was created for the sample and for the negative control (Eqs. A1-A2), setting the 'a' and 'b' parameter values to the number of variant reads and number of reference reads, respectively. Next, the Weitzman overlapping coefficient [17] (Eq. A3) was used to measure the similarity between the sample and negative control distributions to create a significance value. In cases where the number of mutant consensus reads was greater than zero but the estimated p-value was also greater than 0.05, we determined the minimum number of mutant consensus reads (given the number of total consensus reads), for which the cumulative binomial distribution is greater than or equal to the error rate of the given sites as determined by the negative control (error-rate = mutant consensus reads in negative control/total consensus reads in the negative control). If the observed number of mutant consensus reads exceeded this value, we considered it to be marginally significant and therefore above the limit of detection (see Supplementary Table 4 for p-values and binomial test results for each panel at each time point). Note that the overlapping coefficient method can result in low p-values (<<0.05) if the sample VAF ≈ negative control VAF and the depth of the negative control is much greater (>100-fold) than the depth of the sample. In such cases, the ctDNA measurement was considered below the limit of detection if the VAF of the sample was equal to or less than that of the negative control (*e.g*. Supplementary Table 4, Patient 2, time point #1).

$$X_{sample} \sim Beta(a_{sample}, b_{sample}) \quad \text{(A1)}$$

$$X_{neg\_ctrl} \sim Beta(a_{neg\_ctrl}, b_{neg\_ctrl}) \quad \text{(A2)}$$

$$\int min[\, f_{neg\_ctrl}(x),\ f_{sample}(x)]\, dx \quad \text{(A3)}$$

Results

Elevated ctDNA levels are associated with recurrence in rectal adenocarcinoma with clinically-useful lead time

Patient 1 is a 33 year old female who presented with cT3N1M0 distal rectal adenocarcinoma and enrolled on an unrelated phase II trial evaluating the efficacy of total neoadjuvant therapy (8 cycles of FOLFOX chemotherapy and long-course chemoradiation) followed by non-operative management for clinical complete responders based on MRI and endoscopy (NCT02008656) [13]. Whole exome sequencing (WES) of a pretreatment tissue biopsy revealed 81 non-synonymous single nucleotide variants (SNVs, Supplementary Table 3). DIDA-Seq of 28 loci was used to monitor ctDNA levels throughout the patient's treatment course. CtDNA levels decreased 5-fold during four months of total neoadjuvant therapy (Fig 2A). She was without clinically detectable disease for six months following total neoadjuvant therapy and proceeded with NOM per the trial; however, ctDNA levels remained elevated. Eleven months following total neoadjuvant therapy, endoscopic surveillance revealed a biopsy-confirmed recurrence and the patient underwent salvage total mesorectal excision (TME).

Patient 2 is a 59 year old male who presented with cT2N1M0 mid-rectal adenocarcinoma and also enrolled on the aforementioned phase II study. WES of this patient's tumor biopsy found 106 total non-synonymous SNVs and 35 sites were used to assess ctDNA levels in blood draws. At baseline and following total neoadjuvant therapy, ctDNA levels were not considered significantly above negative control, however mutant reads were present (Fig 2B). Similarly, this patient also proceeded with NOM given clinical complete response seen on endoscopy and imaging. However, ctDNA levels were detectable 8 months following the completion of total neoadjuvant therapy, further increased one month prior to biopsy-proven local recurrence, and continued to rise until the time of salvage TME.

Following TME, ctDNA levels again returned to below the limits of detection in spite of later oligometastatic progression. Unfortunately, the performance of this patient's capture panel in the negative control was the lowest of all five panels which resulted in decreased overall sensitivity at the time of oligometastatic progression (see Supplementary Table 2, "Aggregate error rate (%)").

CtDNA levels are associated with tumor burden and progression in oligometastatic esophageal cancer

Patient 3 is a 72 year old male with oligometastatic esophageal cancer who presented with metastatic disease 2 years prior and had received extensive therapy under an immunotherapy trial. Given oligoprogression at the primary site only (distal esophagus), tumor board recommendations were for the patient to undergo neoadjuvant therapy prior to esophagectomy, at which time he was enrolled on our feasibility study. WES revealed significant intertumoral heterogeneity with only 45% of mutations shared and panel sites were selected to represent both shared and private mutations. Using DIDA-Seq, we assessed 17 mutations found only in the primary tissue biopsy and 14 mutations shared between that tumor and a subsequent metastasis (Fig 3). Increasing ctDNA levels throughout neoadjuvant therapy were consistent with clinical non-response. CtDNA levels became undetectable post-esophagectomy but were again elevated seven months following surgery, concordant with clinical progression.

Undetectable ctDNA is associated with pathologic complete response (pCR) following tri-modality therapy for esophageal adenocarcinoma

Patient 4 is a 61 year old male with a history of cT2N0M0 distal esophageal adenocarcinoma who underwent neoadjuvant chemoradiation and esophagectomy. WES revealed 585 non-synonymous mutations and 39 sites were interrogated in blood draws by our capture panel. CtDNA levels declined during neoadjuvant therapy, associated with reduced tumor size and avidity on PET-CT, and were near the limit of detection (*i.e.*, indeterminate as compared negative control values, see Methods) with 5 mutant reads in 114k total reads immediately prior to surgery, and 29 mutant reads in 137k total reads immediately following surgery (Fig 4A). Surgical pathology confirmed a pCR and ctDNA levels remained undetectable as compared to the negative control at final follow-up 6 weeks following his esophagectomy.

Patient 5 is a 69 year old male with cT3N0M0 distal esophageal adenocarcinoma who received neoadjuvant chemoradiation prior to esophagectomy with surgical pathology confirming a near-complete response. WES found 135 non-synonymous mutations and 41 genomic site were included in the ctDNA panel. As with Patient 4, ctDNA levels in this patient were elevated prior to treatment, but quickly fell below the limit of detection during chemoradiation with concurrent reduced tumor size and avidity on PET-CT. CtDNA levels remained statistically insignificant at final follow-up 10 weeks following esophagectomy with no clinical evidence of disease at that time (Fig 4B). Eight months later, the patient was found to have a malignant pleural effusion; however plasma was unable to be collected to evaluate the recurrence of ctDNA.

Discussion

Here, we have demonstrated the feasibility of using patient- and tumor-specific ctDNA monitoring throughout neoadjuvant therapy and surveillance, identifying that such an assay may have the potential to detect sub-clinical disease and more precisely select candidates for organ preservation or those who

may benefit from early salvage resection. Given the morbidity and mortality of large oncologic surgeries, notably esophagectomy, non-operative management for complete responders to neoadjuvant therapy is intriguing and is an active area of investigation [1,18]. Current standard of care for locally-advanced esophageal or rectal cancer consists of neoadjuvant therapy followed by planned surgical resection irrespective of response or biomarker readout. Up to 50% of esophageal squamous cell carcinoma patients exhibit a pCR following neoadjuvant chemoradiation. This has been consistently shown to predict for better disease-free survival and overall survival [19-24] with a meta-analysis identifying a 33-36% overall survival benefit when a pCR is achieved [25]. Given the morbidity and mortality associated with esophagectomy [26-28], avoidance of resection is desirable in those who are at low risk for having residual disease. Furthermore, there is growing evidence in the rectal cancer literature that regimented clinical assessment of patients following neoadjuvant chemoradiation can potentially identify those who are clinical complete responders, allowing avoidance of immediate surgery [29-31]. A multicenter U.S. trial has recently presented preliminary findings testing this hypothesis [18].

Many providers are reluctant to adopt this approach broadly given the poor sensitivity and specificity of clinical response assessments. Current post-neoadjuvant clinical assessment for both esophageal and rectal cancers consists only of direct endoscopic visualization and anatomic/functional imaging (CT, PET/CT, MRI). These tests have difficulty differentiating small regions of treatment-related inflammation or fibrosis from persistent tumor and vice-versa. Multiple studies have examined the concordance rates between these tests and pathology specimens, none of which have exhibited sufficient sensitivity or specificity to accurately identify true complete responders. In rectal cancer, functional MRI has shown great promise with a substantial improvement in sensitivity and specificity (~85% for both) [32]. However, in esophageal cancer assessment of complete response is considerably poor where a combination of endoscopic ultrasound and PET/CT yields only a specificity of 30% [33].

Moreover, as lymph node metastases are still identified in up to 8% of patients with pCR of the primary tumor [34], a more robust and unambiguous biomarker for assessment of complete clinical response is needed and will drastically impact treatment decision making.

There are limited published data on ctDNA quantification during and after neoadjuvant therapy and its correlation with treatment response and suitability for surgery [4]. CtDNA has been shown useful in the detection of minimal residual disease following breast conservation therapy for women with early-stage breast cancer, with detection of ctDNA in plasma after completion of curative therapy predicting metastatic relapse with high accuracy [35]. In a similar study for Stage II and III rectal cancer patients receiving tri-modality therapy with planned surgery, the presence of tumor-specific ctDNA during post-neoadjuvant chemoradiation was highly predictive for disease recurrence despite adjustment for stage, CEA levels and use of adjuvant therapy [36]. Additionally, in a heterogeneous cohort of esophageal cancer patients receiving chemoradiation either in the neoadjuvant or definitive setting, post-chemoradiation panel-based mutation detection of ctDNA was associated with tumor progression, metastasis and shorter survival [37]. The feasibility of our patient- and tumor-specific ctDNA assay in this cohort of patients undergoing neoadjuvant therapy for rectal and esophageal cancer further adds to this body of literature and its potential impact as a useful response assessment biomarker.

There are some limitations to our ctDNA methodology, however. The DIDA-Seq method we have utilized achieves high sensitivity by sequencing select sites to great depth with UMI-based error correction. Consequently, three limiting factors must be considered: 1) hypermutated source tissue, 2) tumor heterogeneity, and 3) variability in performance between selected loci. In Patient 3, mutations shared between the primary and subsequent metastasis were 20-fold more prevalent than those private to the primary and therefore easier to detect. However, a clinical application of our assay for monitoring ctDNA would typically be limited to the mutations found only in the initial tissue biopsy. This highlights

the importance of designing patient panels that are representative of both treatment-responsive and treatment-resistant cancer cell populations. Furthermore, poor site selection may contribute to high, panel-specific error-rates as seen in Patient 2, which had the worst performing panel of all five patients (Supplementary Table 2). For example, it is possible that mutant reads found in this patient at time points prior to surgery, which were determined to be below the panel's limit of detection, were indeed true positives and thus would have provided additional clinical lead time. As sequencing costs decrease, it may be feasible to routinely monitor cfDNA for every mutation identified by exome- or whole-genome sequencing of tumor biopsies, potentially mitigating such issues.

In this feasibility study, patient- and tumor-specific ctDNA analysis throughout multi-modality therapy for esophageal and rectal cancer patients was shown to be feasible and potentially of use in assessment of treatment response. Further investigation with a larger and more homogenous cohort is warranted.

References

1. Noordman BJ, Wijnhoven BPL, Lagarde SM, et al. Neoadjuvant chemoradiotherapy plus surgery versus active surveillance for oesophageal cancer: A stepped-wedge cluster randomised trial. *BMC Cancer.* 2018;18(1):142. doi: 10.1186/s12885-018-4034-1.

2. van der Valk MJM, Hilling DE, Bastiaannet E, et al. Long-term outcomes of clinical complete responders after neoadjuvant treatment for rectal cancer in the international watch & wait database (iwwd): An international multicentre registry study. *Lancet.* 2018;391(10139):2537-2545. doi: 10.1016/S0140-6736(18)31078-X.

3. Markar SR, Karthikesalingam A, Thrumurthy S, Low DE. Volume-outcome relationship in surgery for esophageal malignancy: Systematic review and meta-analysis 2000-2011. *J Gastrointest Surg.* 2012;16(5):1055-1063. doi: 10.1007/s11605-011-1731-3.

4. Reece M, Saluja H, Hollington P, et al. The use of circulating tumor DNA to monitor and predict response to treatment in colorectal cancer. *Front Genet.* 2019;10:1118. doi: 10.3389/fgene.2019.01118.

5. Wan JCM, Heider K, Gale D, et al. Ctdna monitoring using patient-specific sequencing and integration of variant reads. *Sci Transl Med.* 2020;12(548). doi: 10.1126/scitranslmed.aaz8084.

6. Zviran A, Schulman RC, Shah M, et al. Genome-wide cell-free DNA mutational integration enables ultra-sensitive cancer monitoring. *Nat Med.* 2020. doi: 10.1038/s41591-020-0915-3.

7. Cervena K, Vodicka P, Vymetalkova V. Diagnostic and prognostic impact of cell-free DNA in human cancers: Systematic review. *Mutat Res.* 2019;781:100-129. doi: 10.1016/j.mrrev.2019.05.002.

8. Merker JD, Oxnard GR, Compton C, et al. Circulating tumor DNA analysis in patients with cancer: American society of clinical oncology and college of american pathologists joint review. *J Clin Oncol.* 2018;36(16):1631-1641. doi: 10.1200/JCO.2017.76.8671.

9. Lee RJ, Gremel G, Marshall A, et al. Circulating tumor DNA predicts survival in patients with resected high-risk stage ii/iii melanoma. *Ann Oncol.* 2018;29(2):490-496. doi: 10.1093/annonc/mdx717.

10. Zheng D, Ye X, Zhang MZ, et al. Plasma egfr t790m ctdna status is associated with clinical outcome in advanced nsclc patients with acquired egfr-tki resistance. *Sci Rep.* 2016;6:20913. doi: 10.1038/srep20913.

11. Butler TM, Boniface CT, Johnson-Camacho K, et al. Circulating tumor DNA dynamics using patient-customized assays are associated with outcome in neoadjuvantly treated breast cancer. *Cold Spring Harb Mol Case Stud.* 2019;5(2). doi: 10.1101/mcs.a003772.

12. Cibulskis K, Lawrence MS, Carter SL, et al. Sensitive detection of somatic point mutations in impure and heterogeneous cancer samples. *Nat Biotechnol.* 2013;31(3):213-219. doi: 10.1038/nbt.2514.

13. Sequence read archive (sra) [internet]. Bethesda (MD): National library of medicine (US), national center for biotechnology information; 2009 - [cited 2020 may 5]. Available from: https://www.ncbi.nlm.nih.gov/sra/.

14. Ramos AH, Lichtenstein L, Gupta M, et al. Oncotator: Cancer variant annotation tool. *Hum Mutat.* 2015;36(4):E2423-2429. doi: 10.1002/humu.22771.

15. Robinson JT, Thorvaldsdottir H, Wenger AM, Zehir A, Mesirov JP. Variant review with the integrative genomics viewer. *Cancer Res.* 2017;77(21):e31-e34. doi: 10.1158/0008-5472.CAN-17-0337.

16. Kennedy SR, Schmitt MW, Fox EJ, et al. Detecting ultralow-frequency mutations by duplex sequencing. *Nat Protoc.* 2014;9(11):2586-2606. doi: 10.1038/nprot.2014.170.

17. Montoya JA, P GF, González-Sánchez D. Statistical inference for the weitzman overlapping coefficient in a family of distributions. *Applied Mathematical Modelling.* 2019;71:558-568. doi: 10.1016/j.apm.2019.02.036.

18. Garcia-Aguilar J, Patil S, Kim JK, et al. Preliminary results of the organ preservation of rectal adenocarcinoma (opra) trial. *Journal of Clinical Oncology.* 2020;38(15_suppl):4008-4008. doi: 10.1200/JCO.2020.38.15_suppl.4008.

19. Rohatgi PR, Swisher SG, Correa AM, et al. Failure patterns correlate with the proportion of residual carcinoma after preoperative chemoradiotherapy for carcinoma of the esophagus. *Cancer.* 2005;104(7):1349-1355. doi: 10.1002/cncr.21346.

20. Urba SG, Orringer MB, Turrisi A, Iannettoni M, Forastiere A, Strawderman M. Randomized trial of preoperative chemoradiation versus surgery alone in patients with locoregional esophageal carcinoma. *J Clin Oncol.* 2001;19(2):305-313. doi: 10.1200/JCO.2001.19.2.305.

21. Ancona E, Ruol A, Santi S, et al. Only pathologic complete response to neoadjuvant chemotherapy improves significantly the long term survival of patients with resectable esophageal squamous cell carcinoma: Final report of a randomized, controlled trial of preoperative chemotherapy versus surgery alone. *Cancer.* 2001;91(11):2165-2174. https://www.ncbi.nlm.nih.gov/pubmed/11391598.

22. Berger AC, Farma J, Scott WJ, et al. Complete response to neoadjuvant chemoradiotherapy in esophageal carcinoma is associated with significantly improved survival. *J Clin Oncol.* 2005;23(19):4330-4337. doi: 10.1200/JCO.2005.05.017.

23. Chirieac LR, Swisher SG, Ajani JA, et al. Posttherapy pathologic stage predicts survival in patients with esophageal carcinoma receiving preoperative chemoradiation. *Cancer.* 2005;103(7):1347-1355. doi: 10.1002/cncr.20916.

24. Kleinberg L, Knisely JP, Heitmiller R, et al. Mature survival results with preoperative cisplatin, protracted infusion 5-fluorouracil, and 44-gy radiotherapy for esophageal cancer. *Int J Radiat Oncol Biol Phys.* 2003;56(2):328-334. doi: 10.1016/s0360-3016(02)04598-4.

25. Scheer RV, Fakiris AJ, Johnstone PA. Quantifying the benefit of a pathologic complete response after neoadjuvant chemoradiotherapy in the treatment of esophageal cancer. *Int J Radiat Oncol Biol Phys.* 2011;80(4):996-1001. doi: 10.1016/j.ijrobp.2010.03.003.

26. Bailey SH, Bull DA, Harpole DH, et al. Outcomes after esophagectomy: A ten-year prospective cohort. *Ann Thorac Surg.* 2003;75(1):217-222; discussion 222. doi: 10.1016/s0003-4975(02)04368-0.

27. Biere SS, Maas KW, Cuesta MA, van der Peet DL. Cervical or thoracic anastomosis after esophagectomy for cancer: A systematic review and meta-analysis. *Dig Surg.* 2011;28(1):29-35. doi: 10.1159/000322014.

28. Kuo EY, Chang Y, Wright CD. Impact of hospital volume on clinical and economic outcomes for esophagectomy. *Ann Thorac Surg.* 2001;72(4):1118-1124. doi: 10.1016/s0003-4975(01)02962-9.

29. Habr-Gama A, Gama-Rodrigues J, Sao Juliao GP, et al. Local recurrence after complete clinical response and watch and wait in rectal cancer after neoadjuvant chemoradiation: Impact of salvage therapy on local disease control. *Int J Radiat Oncol Biol Phys.* 2014;88(4):822-828. doi: 10.1016/j.ijrobp.2013.12.012.

30. Maas M, Beets-Tan RG, Lambregts DM, et al. Wait-and-see policy for clinical complete responders after chemoradiation for rectal cancer. *J Clin Oncol.* 2011;29(35):4633-4640. doi: 10.1200/JCO.2011.37.7176.

31. Smith JD, Ruby JA, Goodman KA, et al. Nonoperative management of rectal cancer with complete clinical response after neoadjuvant therapy. *Ann Surg.* 2012;256(6):965-972. doi: 10.1097/SLA.0b013e3182759f1c.

32. Gollub MJ, Gultekin DH, Akin O, et al. Dynamic contrast enhanced-mri for the detection of pathological complete response to neoadjuvant chemotherapy for locally advanced rectal cancer. *Eur Radiol.* 2012;22(4):821-831. doi: 10.1007/s00330-011-2321-1.

33. Cheedella NK, Suzuki A, Xiao L, et al. Association between clinical complete response and pathological complete response after preoperative chemoradiation in patients with gastroesophageal cancer: Analysis in a large cohort. *Ann Oncol.* 2013;24(5):1262-1266. doi: 10.1093/annonc/mds617.

34. Tranchart H, Lefevre JH, Svrcek M, Flejou JF, Tiret E, Parc Y. What is the incidence of metastatic lymph node involvement after significant pathologic response of primary tumor following neoadjuvant treatment for locally advanced rectal cancer? *Ann Surg Oncol.* 2013;20(5):1551-1559. doi: 10.1245/s10434-012-2773-9.

35. Garcia-Murillas I, Schiavon G, Weigelt B, et al. Mutation tracking in circulating tumor DNA predicts relapse in early breast cancer. *Sci Transl Med.* 2015;7(302):302ra133. doi: 10.1126/scitranslmed.aab0021.

36. Tie J, Cohen JD, Wang Y, et al. Serial circulating tumour DNA analysis during multimodality treatment of locally advanced rectal cancer: A prospective biomarker study. *Gut.* 2019;68(4):663-671. doi: 10.1136/gutjnl-2017-315852.

37. Azad TD, Chaudhuri AA, Fang P, et al. Circulating tumor DNA analysis for detection of minimal residual disease after chemoradiotherapy for localized esophageal cancer. *Gastroenterology.* 2020;158(3):494-505 e496. doi: 10.1053/j.gastro.2019.10.039.

Figure Captions

Fig 1: Patient treatment and sample collection schema for blood draws and solid tissue biopsies. Solid tissue biopsies were collected after initial diagnosis prior to treatment for whole-exome sequencing (WES). Blood was collected prior to treatment and then at ~1-month intervals during treatment and surgery, and ~3-month intervals during follow-up monitoring. Mutations were called between solid tissue biopsy WES and matched buffy coat WES and used to construct patient-specific sequencing library enrichment panels. Cell-free DNA (cfDNA) isolated from blood draws was sequenced using DIDA-Seq at sites identified in each patient's tumor biopsy to retrospectively determine circulating-tumor DNA (ctDNA) prevalence. *Patient 3 had a solid tissue biopsy of a metastasis which was also analyzed by WES and variants were included in their patient-specific panel.

Fig 2: Rectal cancer patients with detectable post-treatment ctDNA eventually had local recurrence. Serial ctDNA levels were retrospectively analyzed using DIDA-Seq and using patient-specific capture panels. Aggregate variant allele frequency (VAF) was converted to human genome equivalents per ml (hGE/mL) of plasma and plotted over treatment course. (A) A 28-site capture panel was used for Patient 1 and (B) a 35-site capture panel was used for Patient 2. Statistical significance, as compared to a negative control, was determined at each time point. CtDNA values not significantly different from negative controls are indicated (triangle) and aggregate mutant reads/total reads are reported. Statistical significance was determined prior to converting aggregate VAF to hGE/mL plasma.

Fig 3: Oligometastatic esophageal adenocarcinoma cancer patient with primary-only oligoprogression had elevated ctDNA levels associated with systemic disease progression. In Patient 3, whole-exome sequencing of both the primary tissue biopsy and a subsequent metastatic dermal lesion revealed a high mutation burden and 45% overlap in mutation profiles. Serial ctDNA levels were retrospectively analyzed using DIDA-Seq and using patient-specific capture panels. Aggregate variant allele frequency (VAF) was converted to human genome equivalents per ml (hGE/mL) of plasma and plotted in log10-scale over treatment course. Plot shows ctDNA monitoring using mutations either private to the primary tissue biopsy (n=17, solid black line) or shared between the primary tissue biopsy and the biopsy of the metastatic dermal lesion (n=14, dashed red line). Statistical significance, as compared to a negative control, was determined at each time point. CtDNA values not significantly different from negative controls are indicated (triangle) and aggregate mutant reads/total reads are reported. Statistical significance was determined prior to converting aggregate VAF to hGE/mL plasma.

Fig 4: Esophageal adenocarcinoma cancer patients had significant declines in ctDNA during and following neoadjuvant chemoradiation. Patient 4 (A) had surgical confirmation of pathologic complete response (pCR) and Patient 5 (B) had near complete response (CR). Serial ctDNA levels were retrospectively analyzed using DIDA-Seq and using patient-specific capture panels. Aggregate variant allele frequency (VAF) was converted to human genome equivalents per ml (hGE/mL) of plasma and plotted over treatment course. A 39-site capture panel was used for Patient 4 and a 41-site capture panel was used for Patient 5. 18F-FDG-PET/CT showed reduced tumor size and avidity (red arrows) corresponding to near complete response in Patient 5 (B, inset). Statistical significance, as compared to a negative control, was determined at each time point. CtDNA values not significantly different from negative controls are indicated (triangle) and aggregate mutant reads/total reads are reported. Statistical significance was determined prior to converting aggregate VAF to hGE/mL plasma.

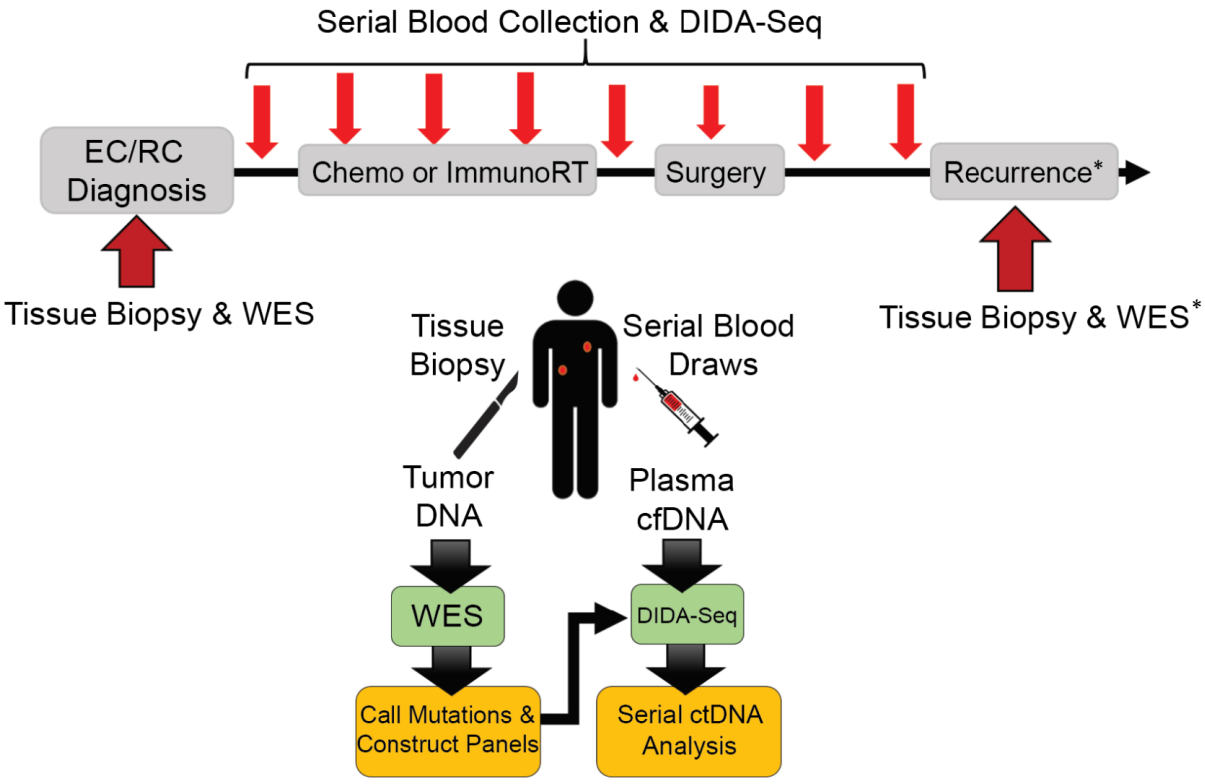

<figure_1.jpg>

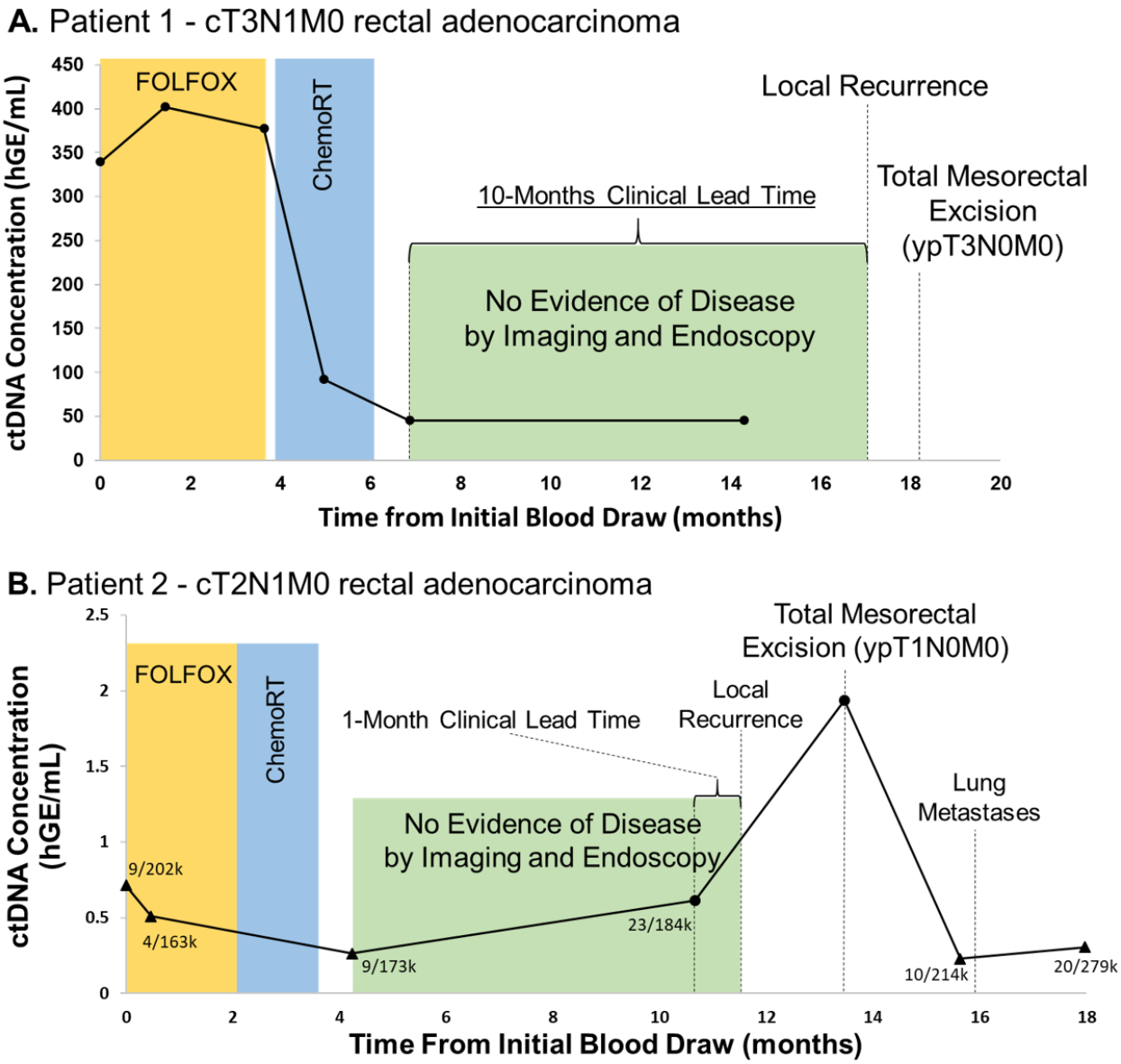

<figure_2.jpg>

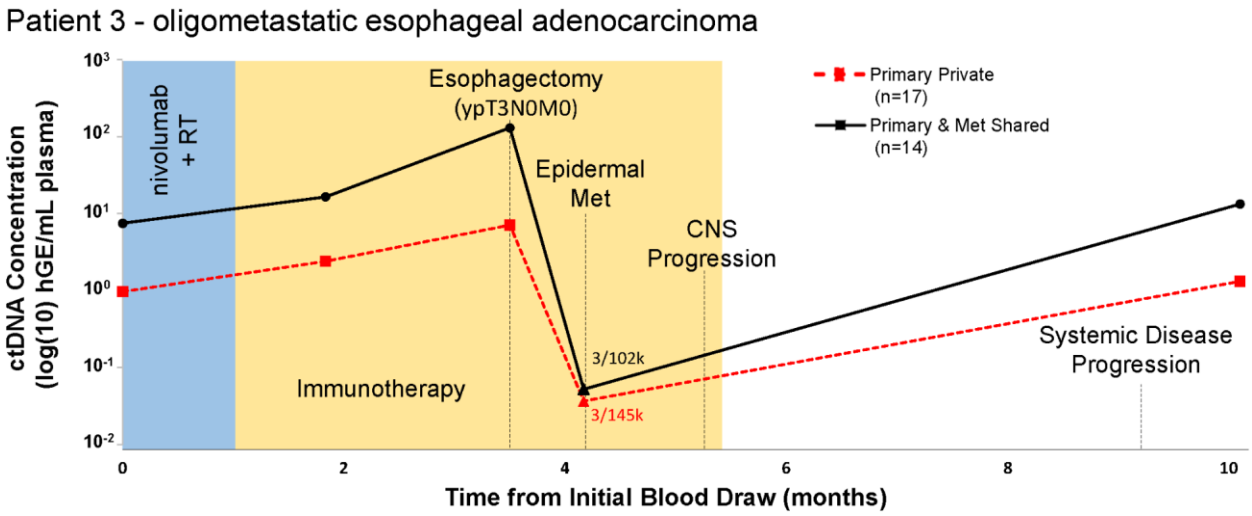

<figure_3.jpg>

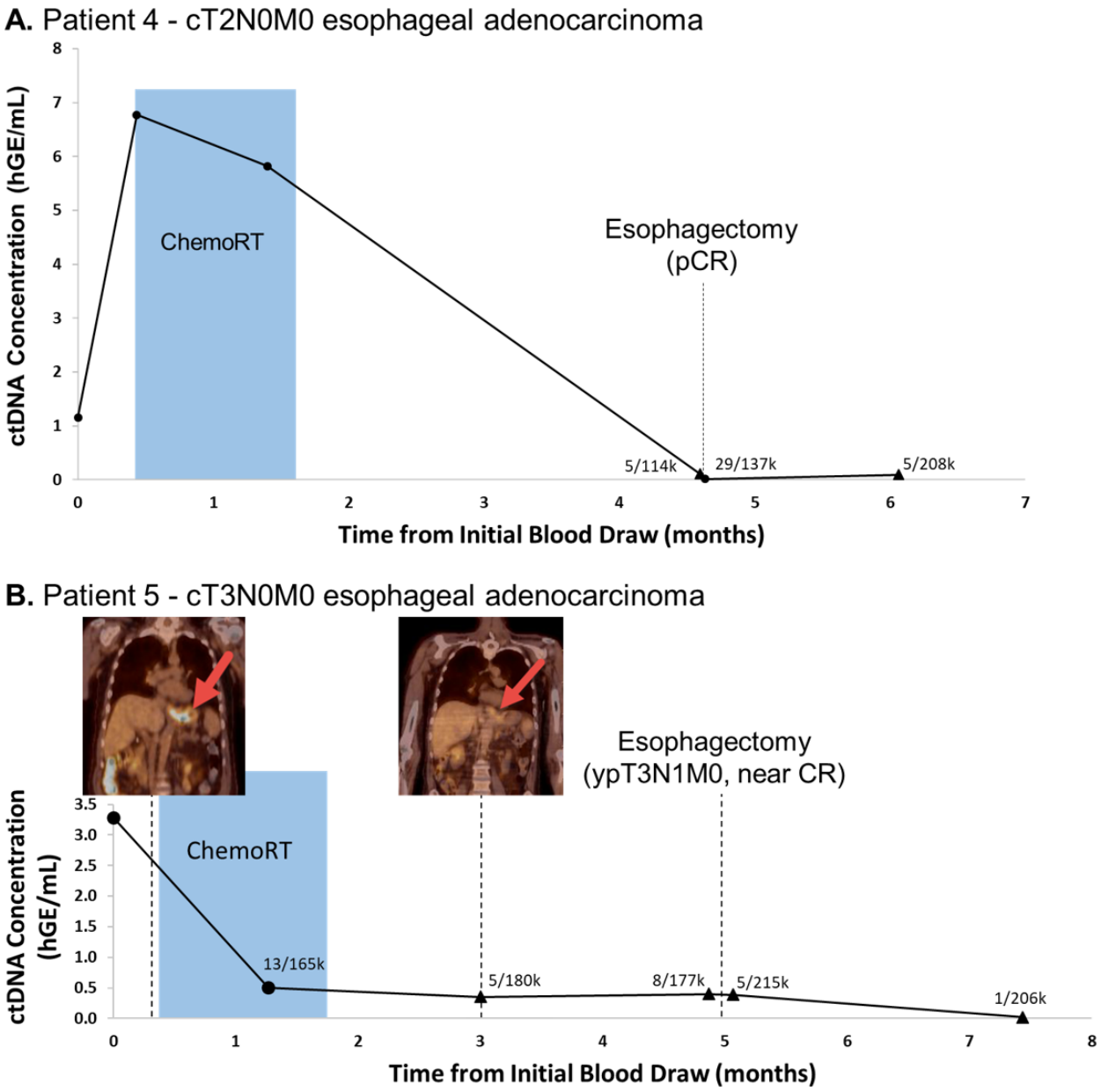

<figure_4.jpg>

Supporting Information

<ECRC_Tables.xlsx>

Supplementary Table S1: Patient-specific hybrid capture targets and bait oligo sequences

Supplementary Table S2: Patient-specific hybrid capture panel evaluation in negative controls

Supplementary Table S3: WES statistics and mutation counts

Supplementary Table S4: DIDA-Seq cfDNA read counts and statistical evaluation

Supplementary Table S1: Patient-specific hybrid capture targets and bait oligo sequences

Patient	chromosome	position	Mutation Call Source	WES VAF	gene	class	bait_oligo_id	bait_oligo_sequence (3'-5')
1	1	3342820	Primary Biopsy	9.6	PRDM16	Intron	TB72B_chr1_3342820	AACCAAGCATCAACGCGAACAGAGAAACGGTAAGAAAACTATCGCGGGCTGGGGAAAGTCTGGACCCGGCCAACAGCCCTGCGTGGCCACCCTCAGAGGACATGCACCTCCACCCCAGC
1	1	201983039	Primary Biopsy	9.4	ELF3	Missense_Mutation	TB72B_chr1_201983039	GAGTTCATCCGGGACATCCTCATCCACCCGGAGCTCAACGAGGGCCTCATGAAGTGGGAGAATCGGCATGAAGGCGTCTTCAAGTTCCTGCGCTCCGAGGCTGTGGCCCAACTATGGGG
1	2	141253099	Primary Biopsy	11.5	LRP1B	Intron	TB72B_chr2_141253099	ATCAAGGAGGAGTGAATTCAATAAGAACGGCTATAAAATTCAGGATCCATATGTATAACTGAGGTTGGATCAGTGGGCAAGTTCAATTCGATACCTGAGAGCGATTTGCAGCCATTTGG
1	2	170058413	Primary Biopsy	9.5	LRP2	Intron	TB72B_chr2_170058413	AGGCTGTCGGTGAGCAGGTGTGAAGTGCTAAGAACAGGAAAAACATGAGAACAAACCCTCTTGATTAAAACATTATCCTAATTTTTAAAAAGATACAATTAAATAAAAGAGACACTTTG
1	2	178562164	Primary Biopsy	13.4	PDE11A	Intron	TB72B_chr2_178562164	AGCTGCATAAGGTCACTATATTCCTTGGAGGACAGGTTAGCAAAGATATTGTGACCCTGTAATGAGAAAGTAAAAAGTCACAAAAGACATTAAATCTGTGGTTGTTGATTACATGTTTT
1	2	220250712	Primary Biopsy	13.1	DNPEP	Missense_Mutation	TB72B_chr2_220250712	ATCCCTCCCAGCCACCGCAGCCCTGCCCCAGTCTCACAGATGCATCTCTGTGTTGGGCCCAAAGTTCTCGTTGATATTTCGCTGCAGATGGATGGCCAGGTGTGGGATGCGAAGAATGG
1	3	127540562	Primary Biopsy	12.4	MGLL	Missense_Mutation	TB72B_chr3_127540562	TGTCACCTGGGGTGACTTTCTGGGGAAGACTTACTTGGGTGTGCCTGTGGGTTTCCAGTACCTGCAGAAGAGGTACTGTCCGTCTGCATTGACCAGGTGAGGGAGGTCCTGGTAGGGAA
1	4	159199550	Primary Biopsy	12.5	RP11-597D13.7	RNA	TB72B_chr4_159199550	ATCTGAATGGCATAGACTTAACTCCTGTGCAAGATACTCCTGTGGCTTCAAGAAAAGAAGATACATATGTTCATTTTAATGTGGACATTGAGCTCCAGAAGCATGTTGAAAAATTAATC
1	6	46649227	Primary Biopsy	9.8	RP11-446F17.3	RNA	TB72B_chr6_46649227	ATATACATGAACATTTTACCCACTCAAGTGTTTTATTATTTCTGAATTTTGAGGAATACATTACTTTCTTCTCTCCCCATACTTTACCCCCAACAGGCTGCTGTGATTGTCAACAGCAG
1	6	57499035	Primary Biopsy	11.0	PRIM2	3'UTR	TB72B_chr6_57499035	TTAGTAAAGGGGACACATTACCAGGTAGCCTGTCAAAAATACTTTGAGATGATACACAATGTAAGTATTTTTTTAACTTTATATCCTAATTATTTGTCTTTTGTTACTGTGTCACATTC
1	6	131996286	Primary Biopsy	14.5	ENPP3	Missense_Mutation	TB72B_chr6_131996286	TGACAGCAATGTATCAAGGTTTAAAAGCCGCTACCTACTTTTGGCCCGGATCAGAAGTGGCTATAAATGGCTCCTTTCCTTCCATATACATGCCTTACAACGGGTAGTGAAGCACTTTC
1	6	152464722	Primary Biopsy	12.7	SYNE1	Intron	TB72B_chr6_152464722	AGACCACATAAAGCCCTGATGCTGCAGACGAACTGTTCTTTGACACAGAACTGTGGTTTCGCACAGGTCGGAATCAGGATGGCCAGGATACTTACGTAGCCTTTGTAGCTGGTGTCTAG
1	7	7917095	Primary Biopsy	9.1	RPA3-AS1	Missense_Mutation	TB72B_chr7_7917095	CCCCGCATGTGCTGGCAGTACAGGGCACCATCACTGACCTTCCCGACCACTTACTCTCCTATGATGGCAGCGAAAACTTATCACGGTTTTGGTATGATTTCACTCTTGAAAATTCAGTG
1	8	62496558	Primary Biopsy	11.4	ASPH	Missense_Mutation	TB72B_chr8_62496558	CTACCCTTTTACGGAGTTTTTCTGCAGCATCAAGTTCAGCTTTAATAGTCTTATCAAATTTATTTAAAAGTTTAGGCTTCTTTTTCTTAACTGAAAGAAAAAAGAGATTTTTATTTTTA
1	8	143857017	Primary Biopsy	12.4	LYNX1	Missense_Mutation	TB72B_chr8_143857017	GAACCTCCCCTTCGTGCTCCCCAGGCAGGGCCACGCAGGGCCCCCAGACTCACAGGTGCGCGTGGTCATGCAGTAGGCAACCATAGCCGGGCAGCGCATGGGGTTGAAGCAGTTGTCTC
1	10	103552679	Primary Biopsy	10.2	MGEA5	Missense_Mutation	TB72B_chr10_103552679	GATAGTATAAACTTTGGAGGTAGGAGTCAGTGGAGGTGGCTGAAAAAAGAGATCATTTGCCCCATCAATTGGCAGCAAACGCTGTGGGAAGAAAAAAAAGGAGATGGATTAGTTTGGGG
1	11	5269572	Primary Biopsy	23.8	HBG1	3'UTR	TB72B_chr11_5269572	GCAGAATAGATTTATTATTTGTATTGCTTGCAGAATAAAGCCTATCCTTGAAAGCTCTGAATCATGGGCAGTGAGCTCAGTGGTATCTGGAGGACAGGGCACTGGCCACTGCAGTCACC
1	11	63998390	Primary Biopsy	10.7	DNAJC4	Missense_Mutation	TB72B_chr11_63998390	CGCCCTTACTGCCCCTGCGCCTGTGCCGGCTGTGGCCCCGCAACCCTCCCTCCCGGCTCCTCGGAGCGGCCGCCGGGCAGCGGTGAGTTGGGCGCGGGGGGCCGGCCCGGTTGTTCAAT
1	12	32893298	Primary Biopsy	10.9	DNM1L	Intron	TB72B_chr12_32893298	ACAGAAAGAACTAAAAGTCTCAAAAACTTACATAACTTTCAGATGTTAAAGCTGCCATTTTAGTGTCACAAAAGTAATATTTTTTCCCCCTCATCCCTATTTAGCCAGTTCCTGTTGCA
1	17	38556545	Primary Biopsy	9.4	TOP2A	Missense_Mutation	TB72B_chr17_38556545	TGGAGTTTGAAGACTTTGTGTAGTCCAACTCTCTCTGCCTCTGCCAGTTTTTCTTCAGTCATCTTCACAACAAATTTCACAGTGGTATCTGTATGGTATTCCCTATAGTCTGTTATGAG
1	17	38556548	Primary Biopsy	9.3	TOP2A	Silent	TB72B_chr17_38556548	AGTTTGAAGACTTTGTGTAGTCCAACTCTCTCTGCCTCTGCCAGTTTTTCTTCAGTCATCTTCACAACAAATTTCACAGTGGTATCTGTATGGTATTCCCTATAGTCTGTTATGAGAGG
1	19	1834985	Primary Biopsy	9.5	REXO1	Intron	TB72B_chr19_1834985	GCTCCCCCACCCTGCAGCCTGTGACCCACTGGTGCTGGAAGGCAGCATCCTGGCCTGGGCGCTCCAGCCAGGTCTGGAAGTTTCACACAGGAAGTTGCCTGGGGCTCGGCCATGGCTGC
1	19	54234420	Primary Biopsy	10.8	MIR518A1	RNA	TB72B_chr19_54234420	TGATGCCGATCGTGGTAATACATTTGCAGAGCATGCTTATCATCAGGCTTGGACAATGCCGGGGTTCTGTTTTCGGTTTTGCTTTTTTATTCTAAGACAGGATCTCTGTTGCCCAGGCT
1	19	54630023	Primary Biopsy	9.9	PRPF31	Intron	TB72B_chr19_54630023	ACAGTTTCCACGAGAGCACAGAAGGGAAGGTGAGGAGGGAAAGGTGAGGGGCGGCCGGGCGTCTTTTCCTCTGGGCCTGGGGTGTCTCTGCAGGGAGACCCTCAGCAGGGAGCCCACCC
1	19	56041241	Primary Biopsy	9.3	SBK2	Silent	TB72B_chr19_56041241	CTGATGGCGATCACAGCGCTCCTCCTTCGGGGGTGAGGGTCCAGCAGCCCCCGCAGAAGCGCGTCGGCCGCGGCGGCCAGGCCGAACCAGGGCTGAGGGCGGTCCCGGGGCTGGCCCGA
1	20	31330940	Primary Biopsy	11.7	COMMD7	Intron	TB72B_chr20_31330940	CCCCTCAGGTGGCCCTTAGGCCTCCGGAGATCCCTTGGCTCCCCACACTCTCCTCAGACCCCAGCTCACCTTAGCCTCGCCCCGAACCCACCTCACACACCCCAAACGCCCACAAGACG
1	20	32439962	Primary Biopsy	11.7	CHMP4B	Missense_Mutation	TB72B_chr20_32439962	AGAAGAACTAGAACAGGAGGAACTAGACAAGAATTTGCTGGAAATCAGTGGACCCGAAACAGTCCCTCTACCAAATGTTCCCTCTATAGCCCTACCATCAAAACCCGGTGAGTGCTTCT
1	X	18841993	Primary Biopsy	15.4	PPEF1	Intron	TB72B_chrX_18841993	TGAGGGAGAGCAGCTGGCCCCATGCTGCCCTGGCTCTCCCAAGGAGGTTGCATTCTTTAAAATCATATTTTAACAAATCATTTGGGCTTTGTTATTGTTGTTGTTAGGAAAACTTTCTG
2	1	1387523	Primary Biopsy	13.8	ATAD3C	Intron	TB80B_chr1_1387523	CGTGCAGAAGCACCATCAGACCTTCTTGGAGTCCATCAGGTGAGCGCTGCCGAGGCCCGGGCCGGCCGCAGATGGAGCCCCCACAGGTGTGAGTCGCTGGTCCCAGGTGCTCTCCAGC
2	1	41157470	Primary Biopsy	21.1	NFYC	5'UTR	TB80B_chr1_41157470	GCTTCGCGCGCGCTCGCCGTTCTCCGTGACGCACACTTCCCCCCTCCCCTCCGCCGCGCCTGGGCCTCTGCATTGCCCGACTCCGTAGGAGCGCGGGGGCGGCTCCTGCTCTTCCTGGACTC
2	1	162353217	Primary Biopsy	22.5	C1orf226	Missense_Mutation	TB80B_chr1_162353217	TGACGTCCCAGCAGACGCTTCACAGCCAGAGGCCACCATGGAAAGAGAAGAGAGAGGCAAAGTTCTGCCCAATGGAGAGGTTTCCCTGTCAGTACCTGACCTAATCCACAAGGATAGCC
2	1	226049907	Primary Biopsy	23.2	TMEM63A	Intron	TB80B_chr1_226049907	AGGGACAGTGAGTTATCTGGAGGGGAACAGGGAGTCAGCCAAGAAGGGGTCTGGATGTGCCTACACTCACTAGGTGGCCATGGACTTCTCCTGGAAGGTGACGAAGGCCATTCCCAGGG
2	5	140431667	Primary Biopsy	18.1	PCDHB1	Missense_Mutation	TB80B_chr5_140431667	TGCAGCCACGGGCCTAAATATGCTGAGCTGGTGCTGAACAAACCCCTGGACCGAGAGGAGCAGCCTGAAGTCAACTTGACAATTACGGCGGTGGACGGCGGGTCCCCGCCTAAGTCTGG
2	6	130392230	Primary Biopsy	17.4	L3MBTL3	Missense_Mutation	TB80B_chr6_130392230	CAAAAAGAATCCCTCATTCATCTGTGTTGCTACGGTAACAGATATGGTGGACAATCGTTTCCTGGTACATTTTGACAACTGGGATGAGAGCTATGACTATTGGTGAGACATTTTCTGTT
2	7	121659278	Primary Biopsy	13.4	PTPRZ1	Silent	TB80B_chr7_121659278	GAGGGGTTGGAATCCGAGAAGAAGGCAGTTATACCCCTTGTGATCGTGTCAGCCCTGACTTTTATCTGTCTAGTGGTTCTTGTGGGTATTCTCATCTACTGGAGGTAAGTTGAGTATTT
2	8	74658997	Primary Biopsy	14.1	STAU2	Intron	TB80B_chr8_74658997	GGCTCCCCAGCGCCCTCTGCCTTCTTCGCCGGCGGCGCGGAAGTCGGGGTCTCCCGGACGCCCCCGATGAGGGTATTTACCTTCTTGCCGGGGACACTTTGCAGACGGCTCCAACATTG
2	9	98056661	Primary Biopsy	17.9	FANCC	Intron	TB80B_chr9_98056661	CTGAGCCAGTCTTGGAGTCACTGGACACAGAGACTCAAACGGACTTCTTACTCGCAGATACCTCTGCTCAGTCCTATGGGTGTAGGGGAAATTCTAACTTCTTAGGCCTTGAGATGTTT
2	9	121976282	Primary Biopsy	22.9	BRINP1	Silent	TB80B_chr9_121976282	TCGGCCCAAGACTTGGCCATGTTGGCCAGCGTGTACTCCATGATCTGGATGTCCGTGATGGGGCAGTTGCACTGCGGAAACTCCTCGGCACATTGGCAGCGACACTGGCTGTTCTGGCA
2	9	136594799	Primary Biopsy	17.2	SARDH	Intron	TB80B_chr9_136594799	CAATCCCCATTTCACAGATGAGGTGACTGAGGCTTGGGGCAGTGAGGGGACCCACAAGGGTCACACCACCTGGGTTCAAGCTGGGATTCAGAGCCAGGTCTCTGTGCCCCCCACAGACT
2	9	137687132	Primary Biopsy	15.5	COL5A1	Missense_Mutation	TB80B_chr9_137687132	CTTGAGCTGACCTTCCTTCTCTCCCATCTGTCCAGGGTCCGAGGGGTGAAAGAGGCCCCCGGGGCATCACTGGGAAGCCTGGCCCCAAGGTATGTTTTTGGCCTCCTGGGCGGTGGGCG
2	11	102713322	Primary Biopsy	23.1	MMP3	Intron	TB80B_chr11_102713322	GCAGAATCAACAGCATCTTTTGGCAAATCTGGTGTATAATTCACAATCCTGTAGGAGAAAAATTGAAGCAGATGCTATTTTCTCCTATGATATAGTTTATAAAATTCCAATCTTATGTG
2	12	14924071	Primary Biopsy	22.6	HIST4H4	5'Flank	TB80B_chr12_14924071	CAGACATTCTGAAATCACAGCGCCTACTCAGCAGAAAATCGGGCTGCCCACTGTGATTGCCAGTCGCAGACCAGGGCTTATAGTCTCTCGATGCGGACCTGTTTGAAAACATCAAAAAA
2	12	31279495	Primary Biopsy	13.3	Unknown	IGR	TB80B_chr12_31279495	AGAGCAGGAAACTGTTGGTCAGGAAGAAGAATCATATATTGTAAACTGATACCCGAACATTCCATGAACTTGTTGAACATTTAAACTAATCATTGTTTATAATATATATAATATATCCT
2	13	26165460	Primary Biopsy	27.0	ATP8A2	Intron	TB80B_chr13_26165460	CATCTTCCCAAACCAAAATTCTGTGCCCCTTTGAACAACTACTCTCCATTCCCACACCTACCTCATCCCCTGGCAGTCATTCTGCTTTGTGTCTCTATGAATTTCACAGCTGTAAGTAC
2	13	31821235	Primary Biopsy	16.1	B3GALTL	Splice_Site	TB80B_chr13_31821235	TCCTCCTTCATCAGCTGGCTAAACAAGAAGGTGCATGGACCATACTTCCGTTGTTACCGCAGTACGTTTGTTTAACTCACCTGTGAATTACTGACATTCCTACCTGAACACTTTTACGC
2	13	38211602	Primary Biopsy	29.5	TRPC4	Missense_Mutation	TB80B_chr13_38211602	CAATTGCTGCTGATCTCGGATGAATCAGGGTGGTTAAATCAAAAAGGCTGAAATTCTTTTTCTTGTCCTTGCTATTACCTTCGCTATCACTCTTTTCATCTGAGTCTGCCGAATTTGAA
2	14	60519822	Primary Biopsy	21.4	LRRC9	Nonsense_Mutation	TB80B_chr14_60519822	TTATTTTTAACTTTATTCAGATTTGTAGAAAAATGCTACATCGCCACATGCTTATATTTCGACTGCCTAACTTACAGATGTTAGATGGAAGTCCTGTGAATTCAGATGATAGGGCAAAA
2	15	73615423	Primary Biopsy	28.9	HCN4	Missense_Mutation	TB80B_chr15_73615423	CTCCTCGGGGAGTAAAGCCTACAGGGGAAGCCCCCCAGAGGCCCCTGCCACAAGGGACGGCGGCTCAGGCTGCCGTGGGGGTGTCTCTGGCGTGCTCAGTGGGCCAGTGGCCAGACCT
2	15	76077931	Primary Biopsy	18.9	RP11-24M17.5	RNA	TB80B_chr15_76077931	GAGGAGGCGCCTCGGCCCACGCCAAACATCCCAGAGGACCTGGAGAGCCGGGAGGCCCACGGTGAGCCTGACTTTCCCTGCCCCGCTTTGCCACCTTCCTCTGTGGTCCCTCCCAGACCC
2	16	71103154	Primary Biopsy	12.8	HYDIN	Intron	TB80B_chr16_71103154	CCCTAGATGAGGGCCCATGACTATTTTGAAGGCTCAGCTGCTTAGCTGTGTGTGCAGGAAGGCCATGCACTTTACCCTGATAGCAGCAAATCCCTGGGGGCGAATGGTGCCACAGTCAG
2	17	7578406	Primary Biopsy	24.5	TP53	Missense_Mutation	TB80B_chr17_7578406	GTCTCTCCAGCCCCAGCTGCTCACCATCGCTATCTGAGCAGCGCTCATGGTGGGGGCAGCGCCTCACAACCTCCGTCATGTGCTGTGACTGCTTGTAGATGGCCATGGCGCGGACGCGG
2	17	7843145	Primary Biopsy	25.0	CNTROB	Intron	TB80B_chr17_7843145	AGAGCTGAGGAACTAGGGAGTAGATGAAGGGCAAAATAATTGAATGGGATGGAATGTTAGAATATGGGGGATACATATAGGCAGGAATGGAGAGTAGAGAGCCATGTGTGGGAGACAAG
2	17	16120857	Primary Biopsy	28.1	PIGL	Intron	TB80B_chr17_16120857	ATGGGAGCCGGGGCTTTGAAAGGGATTTAAGTGCTAACCGATCTCAGTCGCCTTCTTCTCGAAGTTTTCCGTAGGGAGCTAAGTGAATACACCGAAGGTCTTACCTCTGAACCCCTCAC
2	17	18152280	Primary Biopsy	31.1	FLII	Intron	TB80B_chr17_18152280	AGCTGTGATGGTGCATGGGGCAATGGTCACCCCATGCTCCTGACCCCACCAAAAAAAATCCCTCACTATGGGGTTTCTGGGTAAGCCCCAGGGACCCCCCGCCAAGCTCGTGGGCAGGA
2	17	56738199	Primary Biopsy	25.6	TEX14	Intron	TB80B_chr17_56738199	TCATACCAGTCACTCACTGTCATGGAAGCCAGACTTGGATAGCCAGCGCCAAATACTTTGGCTTGCGCCATGTTCCGAGTGAGAATGAAGGGTTTCATTGGAGGCCTCTTCTGGTGACA
2	18	15005666	Primary Biopsy	23.3	Unknown	IGR	TB80B_chr18_15005666	ATCGGGAACAAAGTCCTCCACACTCTGGACTGTTGCTGGGGCCTCTGCGGCTGGGACTGGCTCTGTGAACAGTGATGCTGGGTCCTCTTCACTCGGCACCAGAACCCTCACTGCACCCA
2	18	15005667	Primary Biopsy	22.0	Unknown	IGR	TB80B_chr18_15005667	TCGGGAACAAAGTCCTCCACACTCTGGACTGTTGCTGGGGCCTCTGCGGCTGGGACTGGCTCTGTGAACAGTGATGCTGGGTCCTCTTCACTCGGCACCAGAACCCTCACTGCACCCAA
2	19	14000069	Primary Biopsy	17.0	C19orf57	Missense_Mutation	TB80B_chr19_14000069	TGGGGCTTCGAAGTCAGAGGCGTCCAGGGCATCCTGTATCTGGCTGTCCAGCAGGAAGTCGAGTTCCACAGCTAAAGAGTCTGCCCAGGTGCCCTGGTCTGCAGAATGAGGCAGGTGGT
2	19	50155149	Primary Biopsy	20.5	SCAF1	Silent	TB80B_chr19_50155149	CTGCGCCGCAAGATCCTGACCCAACGGCGGGAGCGCTACCGCCAGCGCTCGCCCTCCCCGGCGCCCCGCGCCCGCCCCGGCCGCCGCTGCTGGTCCGCCCACGCGCAAGAAGTCCAGGCG
2	19	53786160	Primary Biopsy	20.1	FAM90A27P	RNA	TB80B_chr19_53786160	TCCCAGAACTCCCCAAGAGAAAATGCAGGAAGCCTGGAAGGAGCCAGCAGAAGATTGTTTGTTCCTGAGGGTGCGTATTCCCCCGGCCCCTGCTCTGTTTCTCCTCTAGGTCCCCTGAT
2	20	55208532	Primary Biopsy	20.2	TFAP2C	Missense_Mutation	TB80B_chr20_55208532	AATGAACCCCACTGAGGTCTTCTGCTCAGTCCCTGGAAGATTGTCGCTCCTCAGCTCTACGTCTAAATACAAAGTGACAGTGGCTGAAGTACAGAGGCGACTGTCCCCACCTGAATGCT
2	20	60968785	Primary Biopsy	13.0	CABLES2	Intron	TB80B_chr20_60968785	CGCTGCAGGAAGCCCAGACGCACATGCCAGGAGCCCTGCATGGAAAATGAAGGGAACAACTCAGATCAAGCCGTTGAGGCTGCGTCTGAGCTAGACGCTGCTCCTCACATAGCTAGAAC
2	X	91368835	Primary Biopsy	15.2	PCDH11X	Intron	TB80B_chrX_91368835	TCATGAACTTCTTGATCACCTCAAGCACATCAGAAGGCATTGTAGCTGACAGCAAAACTACCTGGGTGTTGCTGTTGAGCTTTTGGAATATGTCATAGATCTGGTCCTTGAATCCACGG
3	1	109394981	Primary Private	46.7	AKNAD1	Silent	TB62B_chr1_109394981	AATGGCTCTTTGGAAAGATGATGAAGTAAAATATCATGACTTGACTTAGAAGCGTCTCCTTCATTTGCTGGAATATGAAGAGCTGCAGTGCATTGTTTCTCTTTCTCGTCTTTTTT
3	2	231406117	Primary Private	47.7	SP100	Intron	TB62B_chr2_231406117	AGCTGCTTTTTCGCCTCAGAACCGTATTATGTAAGTAACAGCCAAACAAAAATGCTTATACTGGCATTTGTCAAATCTGTGATCTGAATCCCATGGCACAAGGTGCCATTCTATTTGGC
3	2	240061281	Primary Private	43.2	HDAC4	Intron	TB62B_chr2_240061281	CAACTGCGTCCTTTTTAGGATGGCTCACAGGCCACTTTCCCTCACCCCAAATTGGAAGGTGAAGAGTGAAGGGCAAGTGCAAAGTGGGGTCATTTCAAGCTCATCCGTCCCGAGTCCGA
3	2	242756299	Primary Private	42.2	NEU4	Missense_Mutation	TB62B_chr2_242756299	GAAGGAACGCCGCGCGCCTCTGCTGTGTGGCCAGCCGTGACGCCGGCCTCTCGTGGGGCAGCGCCCGGGACCTCACCGAGGAGGCCATCGGTGGTGCCGTGCAGGGTAGGCGGGCAGGG
3	3	12299876	Primary Private	43.5	Unknown	IGR	TB62B_chr3_12299876	TACTAGCTTCTGTCATAGTCAGGAGAGTCCCCCATTGTGTACTTCTTTTCCTCGTAGCTTGAGTCTGTGTATTCAAGGAGCAGGTGGATGGCATGTGCCAGCCCGTGGATGTCCCCGTA
3	3	52841810	Primary Private	54.3	ITIH3	Missense_Mutation	TB62B_chr3_52841810	TTCCTCTCGTAGGCTGTCCATGATGATCAACAGGAAGAACATGGTGGTCTCCTTTGGAGATGGGGTTACCTTCGTGGTCGTCCTACACCAGGTGTGGAAGAAACATCCTGTCCACCGTG
3	5	76645440	Primary Private	51.5	PDE8B	Intron	TB62B_chr5_76645440	AAAGGTGGGTTACACCAGCAAAACCAATCCACGAACCCTCTCCCCAATGCACTTTTTTTTCTGAGTTTTAGAATTTCATCCTTAAGATTAGCTTTTTTAATAATGTCATAATTAAGTGA
3	8	26221296	Primary Private	49.5	PPP2R2A	Missense_Mutation	TB62B_chr8_26221296	TGTTTGAAGAACCTGAAGATCCCAGTAACAGGTCATTTTTTCCGAAATCATCTCCTCTATTTCGGATGTAAAATTCAGCCATAGTGGTCGATATATGATGACTAGAGACTATTTGTCA
3	11	57317414	Primary Private	44.4	UBE2L6	IGR	TB62B_chr11_57317414	CATTGCTGGGCTGCCTGCACCCATCCCCTTGGCTCCCATATCCTTCACCTTTGACCTTCTGCTCCTCATTCCACCCCATTCCTTAGGAAACTGGCTGACTGTGCTCAGCTGCTGGACGT
3	12	54448634	Primary Private	48.0	HOXC4	Splice_Site	TB62B_chr12_54448634	TGGGGGGCGGGGAGCCTGCTGCCTCTGAACCCCACTATTTGCTTTCCCCTCCCCCCAGTGAACCCCAATTATAACGGAGGGGAACCCAAGCGCTCGAGGACAGCCTATACCCGGCAGC
3	14	78202265	Primary Private	42.1	SNW1	Intron	TB62B_chr14_78202265	AGGCATAGGGAGGTTATCTATAAAATTAATAACCATGAGTAGAAAAAAATATTTTGGACTACAGCAAAGAATACCTTTCGGCTAGGAGAATGCATGACAGGCGCAGGAGGAGAAGGTGG
3	17	2267302	Primary Private	45.9	SGSM2	Intron	TB62B_chr17_2267302	ACTAGCCTAGCTTGGCCTCCCCTCCTCCCAGCGGGAGCTCATTTCTCATAGGCCATCCCTGAGAGCCTCTCAGCCCTTCATCGTCGGTCTTCCGGTGTCTCCCGCTGTAGAAGGAGGAT
3	19	50399370	Primary Private	43.8	IL4I1	Intron	TB62B_chr19_50399370	CTGGGAGGAGGAGGACAGGGTCAACGGGGTTGTGGCAGGTCGGGGGAGAGGGGTTCTACTCACTTGTTCCAGAGCCCCTCCCCTGCTTACTCACCCAATGGGGCCATGACTCTCGGTGG
3	20	31073595	Primary Private	43.4	C20orf112	5'Flank	TB62B_chr20_31073595	GTTTCCAAACGCGGGAACTGTCCATCCTCACTCTGAAAATGAGATAATTCAGACTCAGGATTTCCCTTTCCCCACCACATTTTCAGAGACCTTTGACTTCTCCTGGCCTGAATTACTAT
3	20	43109010	Primary Private	49.6	TTPAL	Missense_Mutation	TB62B_chr20_43109010	CTGTAGAAGAAGCTGGCCCGAAGTCTTCAATAACTTGAAGCCATCAGCCTTAAAAGATGTCCTTGCTTCCGGGTTCCTCACCGTGCTGCCCCACACTGACCCCAGGGGCTGCCATGTCG
3	21	33076267	Primary Private	42.2	SCAF4	Intron	TB62B_chr21_33076267	TATAATCCCGGAACCTTGTATTCTGGTTTACACTGCAAGGATAAAGATGTAAGATCAGTACAGAAAAAGCAAAGTCACAATCTGACACCCATTATTTTCACATTTATGAAACTTTTATA
3	22	43010677	Primary Private	40.0	POLDIP3	Intron	TB62B_chr22_43010677	GCCTCGGCCAGTGGGCGGGCGGTCGGGGCCACGGCGGGGACGGCGGCAGCCGGCCAATGAGGAGCGCGGCTGTGGTCGGGGGCGGGCGCACCCGGTCCTCCGCGTCGCTCCCGGATCGC
3	2	242814977	Primary & Met Shared	63.3	CXXC11	Missense_Mutation	TB62BE_chr2_242814977	CCCTGCCAGAGACCAATGCTGGTGGCCTCCCCTCCCAGGTCAAGGGCTCCCTTGCCCTCCCCTTCCCTGCTGATGTCCAAGGCAAAGATGCCTTTACTGACATCACTGAAGGCAAAGAG
3	4	57796802	Primary & Met Shared	60.8	REST	Missense_Mutation	TB62BE_chr4_57796802	TTGCATGAAAAAAAGTACAAAGAAGAAAACTCTGAAAAATAAATCAAGTAAGAAAAGCAGTAAGCCTCCTCAGAAGGAACCTGTTGAGAAGGGATCTGCTCAGATGGACCCTCCTCAGA
3	6	167550750	Primary & Met Shared	39.8	CCR6	Silent	TB62B_chr6_167550750	AACTACTTTCTGAAGATCTTGAAGGACCTGTGGTGTGTGAGAAGGAAGTACAAGTCCTCAGGCTTCTCCTGTGCCGGGAGGTACTCAGAAAACATTTCTCGGCAGACCAGTGAGACCGC
3	10	89473851	Primary & Met Shared	68.8	PAPSS2	Silent	TB62BE_chr10_89473851	GCTTTTCAGGATCGTGAGAATGCCCGCAAAATACATGAATCAGCAGGGCTGCCATTCTTTGAAATATTTGTAGATGCACCTCTAAATATTTGTGAAAGCAGAGACGTAAAAGGCCTCTA
3	10	96006346	Primary & Met Shared	60.9	PLCE1	Missense_Mutation	TB62BE_chr10_96006346	TATTGGAACTCACTAGAGCTGTGAGAAAGATGAGGAAATTCCCTGACCAAAGACAGCAGTGGCTGCGGAAACAGTACGTCAGCCTTTATCAGGTAAGGGGTGCAGCCATCCCTCTTTCC
3	12	18641526	Primary & Met Shared	56.5	PIK3C2G	Missense_Mutation	TB62BE_chr12_18641526	AGCCTTGAATGATGAGTTTTCCAAGGAGCAGAAACTTATCAAAATTCTGGGAGATATTGGGGAAAGAGTCAAGTCTGCCAGTGACCATCAAAGACAGGTTTGTTGAAATATTAATATTC
3	12	62147472	Primary & Met Shared	61.7	FAM19A2	Silent	TB62BE_chr12_62147472	TTGACTTTATTCCCAGAGGAACAGCTCCATCCTTTCCGATCCGGAAGGAACTTTACATTCTTCTCCCTCTAGACATGGCTGCATATGGCACCACCATTTCTGTTCCACTATTGAAGCTAT
3	18	32418761	Primary & Met Shared	54.3	DTNA	Missense_Mutation	TB62BE_chr18_32418761	GTTTCAGGATACAGTACAGCCTGAATGTGGCAGACAGGCTAGCTGATGAACATGTTCTCATCGGGTTGTATGTCAACATGCTCCGGAACCAACCCCTCATGGTTAGTGCAGGTTTGGCTG
3	X	49077012	Primary & Met Shared	70.0	CACNA1F	Intron	TB62BE_chrX_49077012	CCTCCTCTTCCTCTTTCTCCACACCAGGCACCTGAGGACAGGAAGACGGGAGTCATCAATGGTGAGGGAGACACAGGGAATGGACACAGGGGAGGCATGGAAGAAATGTAATAATAGGG
3	X	95990776	Primary & Met Shared	77.1	DIAPH2	Missense_Mutation	TB62B_chrX_95990776	TGATGGGTTTTTTTTGTTTGTTTCTTTTTGGTTTTAATAGAACATTCAAATAAAAACTTTGGCAGATGATGTGGTAAGGTGGTCTTAGCATGTTATTACATTACTTATGCATGTTGCCT
3	X	114426912	Primary & Met Shared	71.9	RBMXL3	Missense_Mutation	TB62BE_chrX_114426912	AGGAGTACCGAGGCCCCTCGCCTGACGCCCACAGTGGGGGCCGCGACAGTTCCATCAAGAGTTACGGCCTGAGCGACCGCTACGGAGGAGGAGGCCACTACGAGGAGTACCAGGGCAGC
3	X	130217172	Primary & Met Shared	60.5	ARHGAP36	Missense_Mutation	TB62BE_chrX_130217172	ATCTTTTCTTTTTCTCTTTCTGTAGCTCTGCCTATTGACCGTCCGAACACCTTGGATAAGTGGTTTCTGATTTTGAGAGGACAGCAGAGGGGTGAGGGGGCTCTTGTATTTTCTTTAG
3	X	130220456	Primary & Met Shared	71.1	ARHGAP36	Intron	TB62BE_chrX_130220456	TCCAGTGAGTGTTTTTTGGGTTTGTTTATGCTTAGCCTGAAGTACCTCCTCCTATGGGGTTTTCCAACTCCAGACTATCTTTATATTAAGTAACGCAAGTACACAAACTGACTTTTTCA
3	X	136651102	Primary & Met Shared	54.5	ZIC3	Missense_Mutation	TB62BE_chrX_136651102	GGTTTTTGCCTTTTGCAGGTGAGAAACCTTTCAAATGTGAATTTGAAGGCTGTGACAGACGCTTTGCCAACAGCAGCGACCGTAAGAAGCACATGCATGTGCATACCTCGGACAAGCCC
4	1	11810142	Primary Biopsy	22.0	AGTRAP	Missense_Mutation	TB98B_chr1_11810142	CCGAGTTCTCACCCTTCATTTTTCTTCCCACCATGTCCCCTGTCTACCTAGGTTTCCTTGGGTCTTCTCAGGACCGTAGTGCCTACCAGACGATTGACTCAGCAGAGGCGCCCCGCAGAT
4	1	21890712	Primary Biopsy	18.7	ALPL	Intron	TB98B_chr1_21890712	AGCCAGGGCTGTAAGGACATCGCCTACCAGCTCATGCATAACATCAGGGACATTGACGTGAGTGCTCGGGGGCAGCCGGGCAGGGACGGGGTGAGGCGGGGCCTCTGGTGGGCAGGAGG
4	1	72076694	Primary Biopsy	19.9	NEGR1	Intron	TB98B_chr1_72076694	TAAAGTAAGTATCTGAAACACAAGCACGTTAGCTCAAAGTGCTTAGAACACAGTAATAATCACAAAGTCCTCACTTCTTCTCTCCTTTGTACCATTCAAAGGCTGGAGGCGGCACACCT
4	2	20320736	Primary Biopsy	19.2	Unknown	IGR	TB98B_chr2_20320736	ATGGTTGGCTGTGTCTCTTCATTGAAATAATCTCTTGGTTTCAGAGAAAACAACCTCCTTACTTTTCTTGTCTCTCTTTGCCCATCTCAAGCTCCTCTGTTGGTTTCCATCAACCTCTA
4	3	418101	Primary Biopsy	22.2	CHL1	Intron	TB98B_chr3_418101	CCCATCTCCAAATGTACTGATTTGGAACCTGGACTGAGGCTGGAACACGACATTTTTAATAAGTTCTTTAGGTATACCATACCTACCACATTTCGAGGACTAGTGAGGCACCCAACGTT
4	3	48658299	Primary Biopsy	28.0	TMEM89	Silent	TB98B_chr3_48658299	CTCAGGCTGTCAGGCAAAGAGAGGCACATGTTCGGTCACCCACTCTGGGTGGAAGTCCCCTTTATTTGGATTTGCCGCTGGGTGGCTAGATGACGTAGGTGGCCTTCGATGTGGACCAG
4	4	47034603	Primary Biopsy	18.9	GABRB1	Intron	TB98B_chr4_47034603	ATGGGAAATGGACAGGTCCCTTTGCCCTCTGCGTTTCATTGGCGGTCACCTCGCCCCTGGCCCCTGAGGTCCCACTCCGCACCCGCTCCCCGCTCCGGCACACACACCCGGTCGCCCCT
4	5	155066	Primary Biopsy	20.0	PLEKHG4B	Missense_Mutation	TB98B_chr5_155066	CCTGAAGGCCGTGCACAAATTTGTTGACAGCTGCCAGCTGACCGCAGACCTCGACGGCTCCTTTCCCTACAGCCATGGTGACTGGATCTGCTTCCGTCAGGTAGGTTCAGCCTGCAGCT
4	5	140166575	Primary Biopsy	20.7	PCDHA1	Missense_Mutation	TB98B_chr5_140166575	CCACTGATGGGGGCAAACCGGAGCTGCAAGGTACAGTTGAGCTGCTGATCACCGTCCTCGACGTTAATGATAACGCCCCCACTGTTTGACCAGGCCGTATACAGAGTCCACTTGTTAGAG
4	6	112575299	Primary Biopsy	19.4	LAMA4	Silent	TB98B_chr6_112575299	CCTTCAATGTCAAAAGGAAAAGCGTTGTCGTCCCCGGACGCGGCGCGGGAGCAGGCAGCGCTCCAGAGGAGCCACAGAGGCAGAACCGAGCGCCAGGCTGAGCTCAAAGCCATTTCTCC
4	6	154332232	Primary Biopsy	25.6	OPRM1	Intron	TB98B_chr6_154332232	TTTTGTTGAAGAAATCCTTTTCATTGCATTTGCTGGAAGAGGAGGAGTAAGGGCTGCTTGACACTCATCTCTTAAATGCTATACATTCTACCTTGTCCCTGTGATGTAAGAGCAGGAAA
4	7	100086497	Primary Biopsy	19.1	NYAP1	Missense_Mutation	TB98B_chr7_100086497	AGCCAGCCGGCTCCACCCCAGCTCCCCAAGTGCCTGCACGGGAGCGGAGACGCCTCCCCCACCGCCTCCACCTCCTGCTGCCAACCTGCTGCTGCTGGGACCATCGGGCCGGGCCCGG
4	8	110346275	Primary Biopsy	19.0	ENY2	5'Flank	TB98B_chr8_110346275	GGAGCAATTAGCCGCCACCTCCATCGCTTTCCAGGGCCGCAGCGTGAGAATTAATAAAGCCCTTGTTGAAAGGTCCGCGCTTCACGCCTCGCACAGAGACTGGGAAGCGGCGTGGTTCC
4	9	107546506	Primary Biopsy	19.6	ABCA1	3'UTR	TB98B_chr9_107546506	AATTGCATTGCATTGAATAGTATCAGTACAGTATCCAGTTTACTTCTTCCCACATCAACTTCTGGCTCTTTTCTCCACAACACTTCACATGGTGCAAAGGAAAGTCTAGTTCCTCTTTA
4	10	5808533	Primary Biopsy	20.5	GDI2	Missense_Mutation	TB98B_chr10_5808533	CAAGAGCTCCAAAGCTGGTCTGATTTCCTTCTCAGGCTCCTTGGTTTCCACAGTTGTACTAACTATAGCAATGTACTTCCCTTGTGCTGCTACATTGTGCGCAAAGGAGATCATGCAGA
4	10	73767957	Primary Biopsy	21.0	CHST3	Missense_Mutation	TB98B_chr10_73767957	GCTACGAGGACGTGGCACGCGGGCCGCTGCAGAAGGCCCGCGAGATGTACCGCTTCGCCGGCATCCCCCTGACCCCGCAGGTGGAAGACTGGATCCAAAAGAACACGCAGGCGGCCCAC
4	10	106581899	Primary Biopsy	20.0	SORCS3	Intron	TB98B_chr10_106581899	CTGGAGTCTGACCAGCTCCTCTGTGATTCTTATTTCTCTAGATCAGGAATCTGATCTGTCCTCAGTTTCTGTATCTGTATCTGACAGTCAGGTCTCAGAACTGAGGCCTTAATTCCCAA
4	11	61015688	Primary Biopsy	23.1	PGA5	Intron	TB98B_chr11_61015688	AGTTCCACCACTCCCCCGCTGTGTGACCTTGGGCAGGTGGCCTCACCTCCCTCAGGCTCAGTGTCCTCATGGTAAGTGGAAACAACAGTGACGGTGCCCACTGCATGGGCCCTGGCCTA
4	11	66627309	Primary Biopsy	19.3	LRFN4	Silent	TB98B_chr11_66627309	TCCACGCTGCCGGCCTCGCCCCTGTGCCACGCCCTGCAGGCCCACGTGCTGGGCGGGACCCTGACCGTGGCCGTGGGGGGTGTGCTGGTGGCTGCCTTACTGGTCTTCACTGTGGCCTT
4	12	9313735	Primary Biopsy	32.8	PZP	Intron	TB98B_chr12_9313735	GGGAGCTTCAAGGACAACTGCTCAGACACATTAGCACCTTTAGAAACAGACAGCCCATGTTAAAGGAGGACATCTATGATTACAATATAATTTAGTGATTATAATGTAGTGAGAGCTTC
4	12	51108244	Primary Biopsy	21.6	DIP2B	Missense_Mutation	TB98B_chr12_51108244	ATAGCATTCATCAAGTGGGGGTTTATTGTCTTGCTCTGGTGCCAGCCAATACATTGCCAAAAACTCCACTAGGAGGAATCCATATATCTCAGACGAAACAACTCTTTCTGGAGGGATCA
4	13	65532475	Primary Biopsy	27.6	Unknown	IGR	TB98B_chr13_65532475	TCTCAGACAGGAGCTGCTCCACCTCAGCCTCGGACGCTGCCAGCAAGGAGGCGATCTTGCGCACTGACTTCTCAATGAGGTGCCTGGCATCCAGATGCCGCTGGATCTCCTCTGTGAGC
4	13	103295635	Primary Biopsy	29.2	TPP2	Missense_Mutation	TB98B_chr13_103295635	GACAGTGTGTTCGTGTTCTTCTGAGGTGTCAGCAAAGTTTGTTCTACATGCAGTCCAGCTTGTGAAGCAAAGAGCATATCGAAGCCATGAATTCTATAAGTTTTGTTCTCTTCCAGAGA
4	13	111213867	Primary Biopsy	33.1	RAB20	5'UTR	TB98B_chr13_111213867	GACGTCTTCCCCACGTTCATGTCCCCCAGGAGCACGATCTTGCTGTCGGGCTTCCTCATCTTCCCGTAAGAACCCCCAGCGCCCCCGCGCCCTCTCCCCGAGGCTGGCCGGCTCGTGCG
4	13	113030684	Primary Biopsy	18.7	SPACA7	5'UTR	TB98B_chr13_113030684	TCCACAGTGTCCTGGAGACCAAGGATGGGAAACTGTCAACCTTCAGAACGTCCTTCTCCCTCAGCTGGAGGGAGCATGGCAGTGAGCCAAGGAGACGGGACCCTCTGCTTTGTCCTCCT
4	13	114619131	Primary Biopsy	37.3	LINC00452	lincRNA	TB98B_chr13_114619131	TCTGGGTAGGTAAAGCCCAGGCTAATCGCAGGTTCAGTGACCCGACAGTGCATTTAGGACAGTGATACTAGATGGGACGACCAAGCTCTGTGAGTTACACAATGGGGTGAGTTAGACAG
4	15	75406888	Primary Biopsy	22.4	PPCDC	Intron	TB98B_chr15_75406888	ACAGCTGGTGAGAGGGGAACCCCCATCAAGTGCTGCCAGCCCATCCGGCTGACACATGTCAACACTGGCTGAAACCTCCACAACTTTCTGAAAACCAGGAAGTGGGTGCTTTTGGTGAG
4	15	93518046	Primary Biopsy	32.0	CHD2	Intron	TB98B_chr15_93518046	AGTGCTTTGCAGTTATTTTTACTCAGTGGGTGTTCAGGTGATAAAGGTTCCAAGTCTGCTGTTCTATTCTGAGTGTAGCTGATCTTCCTATCTTACAGTTTTCTTGTGGTTTATTTTTA
4	16	20997064	Primary Biopsy	20.5	DNAH3	Intron	TB98B_chr16_20997064	TATCTTTCCAGTGGGTGACAAGTGGATAAGCACCTGTAAGAAAAGTAAATCTCGGCGGGGCATTCAGTGAATGGCCCAGCCAGGCTGGTAGGGACATCATGGAGGGAGGGCATGGGAGA
4	16	22145622	Primary Biopsy	20.8	VWA3A	Intron	TB98B_chr16_22145622	CAGGAGTAAGCCACCATTCCCAGCCCTCAAGTCACCTCCAGGTGGCTTTCTAGTATCCAGATGATGGGGACGCTTGCCAGGATCCACACCCTGTCTCACCTTGCTCACGATGTGCTTTG
4	16	67236272	Primary Biopsy	19.0	ELMO3	Intron	TB98B_chr16_67236272	ATGGCCAAGAGCAGGGGACGGAAGGGCAGAGAGGGCCAGGGGCTGTATGCACTTTCTCCCTGAGCCCCTCCTGCCCCCCCACTCCAGGCTCTGAGACAGCCCAGGACTTCTCACCCATG
4	17	48606038	Primary Biopsy	26.1	MYCBPAP	Intron	TB98B_chr17_48606038	CAAGCCTCCTCACGTACCTGCAGCATCCACTAGGCTGTTGGGGGCCTGCCATATTTTCTTCCACCCACCTCCCTTAGATCAAAAATCACCTCCTATCATGGAAGTGAAGGTACCTGTGG
4	17	51063078	Primary Biopsy	25.6	C17orf112	Missense_Mutation	TB98B_chr17_51063078	TCTTCAACGGCATCTCTAGCATGTATACTTCCCTTAAATCCACCTTCGTAGCATTTGCTGATGGTAATTCAGGGACTAGAAAAGCAAACTTTTAGAGATTTAATTTTTTTCTTTCTTTC
4	19	7982332	Primary Biopsy	25.3	TGFBR3L	Intron	TB98B_chr19_7982332	GGTCTCTCTTGGGGGCCCTGGGGACCAGAGCCACGATCCCGGTGCCCTGATGTCCCCGTCTCTTCCCCACCTTCCTCTCCCCCAGTGTCTGCCTCAGGACGAGGCGTGCGCCGACACTG
4	19	47177809	Primary Biopsy	25.5	PRKD2	Missense_Mutation	TB98B_chr19_47177809	AGGGCAGCAGCTGGACGAGGGCACAGGACCTCAGAGAACACTGATGCGCTCCGCCAGCCCCTGCATGTCGTGGTCCTGTGGTGGACAGGCCCCACCGAGATCCCTGTCCGTGGGCAGCC
4	20	3732789	Primary Biopsy	23.3	HSPA12B	Silent	TB98B_chr20_3732789	GGCGACACCGAAATTAAGGTCACCGCCGTCGACGTCAGCACCAATCGCTCCGTGCGCGCGTCCATCGACTTTCTTTCCAACTGAGGGCGCGCCGGCGCGGTGCCAGCGCCGTCTGCCCG
4	22	51043138	Primary Biopsy	27.1	MAPK8IP2	Missense_Mutation	TB98B_chr22_51043138	CCGCGCCCGGCCGCGCCGCCCGCCCGGGACGAGCCTGCTCCGCCGCCTGCTCCGAGGAGGAGGACGAAGAGGACGACGAGGAAGAGGAGGATGCCGAGGACAGTGCGGGGTCCCCCGGG
4	X	86082726	Primary Biopsy	21.7	DACH2	Intron	TB98B_chrX_86082726	ATAAAGTGAGTTTGTGGTTTTCAGTGAAGTGCATTGAGTAGATTTTGAATTTTCTTTGTTCGAATGAAATTTTGACCAGGTCTTATTGTTTTTTCTGTGCAGCCTGAACACTGATGCCG
4	X	86082730	Primary Biopsy	20.8	DACH2	Intron	TB98B_chrX_86082730	AGTGAGTTTGTGGTTTTCAGTGAAGTGCATTGAGTAGATTTTGAATTTTCTTTGTTCGAATGAAATTTTGACCAGGTCTTATTGTTTTTTCTGTGCAGCCTGAACACTGATGCCGGAAC
5	1	27022984	Primary Biopsy	8.7	ARID1A	Silent	TB86B_chr1_27022984	AGCAGCCTGGGCAACCCGCCGCCGCCGCCGCCCTCGGAGCTGAAGAAAGCCGAGCAGCAGCAGCAGCGGGAGGAGGCGGGGGGCGAGGCGGCGGCGGCGGCAGCGGCCGAGCGCGGGGAAAT
5	1	27023695	Primary Biopsy	7.4	ARID1A	Silent	TB86B_chr1_27023695	GGCTCCAAGCCGCCTCCCTCCTCCAGCGCCTCCGCCTCCTCGTCGTCTTCGTCCTTCGCTCAGCAGCAGCGCTTCGGGGCCATGGGGGGAGGCGGCCCCTCCGCGGCCGGCGGGGGAACTCC
5	1	113992787	Primary Biopsy	47.9	MAGI3	Intron	TB86B_chr1_113992787	CGGAAGACAGGCAGAGTGGAAAAAGAGGATTTGCTTTTGTAACTTTTGATGAGCATGATACAGTTGATAAAATTGTTGTTCAGAAATACCACACTATTAATGGGCATAATTGTGAAGT
5	1	113992919	Primary Biopsy	44.3	MAGI3	Intron	TB86B_chr1_113992919	TCTAAACAAGAGATGCAGTCTGCTGGATCACAGAGAGGTCGTGGAGGTGGATCTGGCAATTTTATGGGTCGCGGAGGAAACTTTGGAGGTGGTGGAGGAGCTATGGTGGTGGAGGTGGT
5	1	164815949	Primary Biopsy	7.5	PBX1	3'UTR	TB86B_chr1_164815949	GTTCACTCTGATACCTCCAACTGATCTCCCAGCAATCGCATCCCGGCTGACCCTGTGCCCCAGTTGGGGCAGGGGCAGGAGGGAGGGTTTCTCTCCCAACGCTGAAGCGGTCAGACTGG
5	1	176145062	Primary Biopsy	28.6	RFWD2	Silent	TB86B_chr1_176145062	GGATCGAAATATTTTTAAAATAAAAATCATTCCAAAGACTCACCCAAGAAATTAGGATACAGATGGTCAATATTGTCCACAACATAGTTACACTTGGGACATCTATTATTGTCCTCCAA
5	1	176145089	Primary Biopsy	33.9	RFWD2	Silent	TB86B_chr1_176145089	CATTCCAAAGACTCACCCAAGAAATTAGGATACAGATGGTCAATATTGTCCACAACATAGTTACACTTGGGACATCTATTATTGTCCTCCAAACTCTGATGAATACACTTGTAGCTATT
5	2	45861	Primary Biopsy	25.6	FAM110C	Silent	TB86B_chr2_45861	CGACGCCTCACCACCCGCGGCTCTGGCCCAGGGGGCGCGGCCGGGACACTGGAGGGCGCCGCGGACCGCGCGGCTGGGGCTGGGGTCTCGGGGATTGCGGGGTCCGCCGCGGGGCCAGG
5	2	9347305	Primary Biopsy	20.9	ASAP2	Silent	TB86B_chr2_9347305	ATCTCCGTGTCGGAATTCGTGGCCGAGACCCATGAGGACTACAAGGCGCCCACGGCCTCCAGCTTCACCACCCGCACGGCGCAGTGCCGGAACACTGTGGCGGCCATCGAGGAGGTGAG
5	7	27204549	Primary Biopsy	7.1	HOXA9	Silent	TB86B_chr7_27204549	CACTTACTGGGATCGATGGGGGGCTTGTCTCCGCCGCTCTCATTCTCAGCATTGTTTTCAGAGAAGGCGCCTTCGCTGGGTTGTTTTTCTCTATCAACTGGAGGAGAACCACAAGCATA
5	7	148506037	Primary Biopsy	9.7	EZH2	Intron	TB86B_chr7_148506037	GCCTTGTATAATATATAAATGGATAATAAATACATAACAGGAAAGTGTAACCTAATTCCCCACTAATGCTCATGGCAAAGTGACCCATCAAAAGAAGCAAAGAACTAAAAACCCTCCTT
5	11	90016113	Primary Biopsy	19.4	Unknown	IGR	TB86B_chr11_90016113	GTTTGCACTGGCACCTACCGCCAGCTCTTCCACCCTGAGCAGCTCATCACAGGCAAGGAAGATGCTGCCAATAACTATGCCCGAGGGCACTACACCATTGGCAAGGAGATCATTGACCT
5	11	124948872	Primary Biopsy	23.3	SLC37A2	Intron	TB86B_chr11_124948872	CTAAATTCATGGAGCATGGCCAGGTGTCACAGAAGCAGTGGGGGACAGAGGTTGGCCCCGTCACATGGCAACACAGAAGTCATTGGTGGGACCTTGGCCAGAGCCACTTCCTAGCGTGG
5	12	49522215	Primary Biopsy	20.0	TUBA1B	Silent	TB86B_chr12_49522215	GCCATGTATTTACCATGGCGAGGGTCACATTTCACCATCTGGTTGGCTGGCTCAAAGCAAGCATTGGTGATCTCTGCTACAGAAAGCTGTTCATGGTAGGCTTTCTCAGCAGAGATGAC
5	12	121769162	Primary Biopsy	29.5	ANAPC5	Silent	TB86B_chr12_121769162	CAATTCAACCCGTGAACAAAACTCCCAAGACCAGAGGATGGCCTCACCAAACAGTGCTGGAGACACACGTGATCGTTGGACTCCTGGGCAATCCTAATTGCCTCCTGCAGGGCGAGCTC
5	14	36988572	Primary Biopsy	8.6	NKX2-1	5'UTR	TB86B_chr14_36988572	AAGATGTCAGACACTGAGAACGGAGTCGTGTGCTTTGGACTCATCGACATGATTCGGCGGCGGCTGGAGGAGGAAGGAAGAGGAGGAAAAAAAAAGGGAGAGGGGGAAGGCGAAGCCTCG
5	14	36988900	Primary Biopsy	7.9	NKX2-1	Intron	TB86B_chr14_36988900	CCTACATCTTGCCCGAGATAATTAGCTTACATGCTGATGACAAGGTAAACACCTTTAAGTTTCACTTGTCAGGATTTTTAGGTCTCAAAGAGAGAGAGAGAGAGGCAGAGACGAGACCC
5	16	65032706	Primary Biopsy	7.1	CDH11	Silent	TB86B_chr16_65032706	TTGGTGGCATGAATGTTCCCTGATTTGTCATCAATCACAAAAATGGTTCCAGCTCCTTCCCCTGAGAGAATGTATTTAATGTTCCCATCACCAGAGTCAATATCTGAATGAAGCTGGAA
5	17	62496725	Primary Biopsy	8.7	DDX5	Silent	TB86B_chr17_62496725	CCTGAACCTCTGTCTTCGACCAACTGAAGCAACTTGGGATTAATTGCTTGATTAGCTTCACGAAGCACAGAGATAAGGTCGCTCACTTGCTTTATGTTATTAGGTGTAAAGAAAGTGTA
5	21	34400111	Primary Biopsy	23.5	OLIG2	Missense_Mutation	TB86B_chr21_34400111	CTGCAGCATGTGCCAGGTGCCGCCGCCGCGCACCACCACGTGTCGGCTATGGGCGCCGGCAGCCTGCCGCGCCTCACCTCCGACGCCAAGTGAGCCGACTGGCGCCGGCGCGTTCTGGCGA
5	21	34400113	Primary Biopsy	22.9	OLIG2	Silent	TB86B_chr21_34400113	GCAGCATGTGCCAGGTGCCGCCGCCGCGCACCACCACGTGTCGGCTATGGGCGCCGGCAGCCTGCCGCGCCTCACCTCCGACGCCAAGTGAGCCGACTGGCGCCGGCGCGTTCTGGCGACA
5	22	20502716	Primary Biopsy	26.8	Unknown	IGR	TB86B_chr22_20502716	AGGCCCTGCCGGTGCACCACCTTTGTAGCCGGCTCTTGGTGGGATTTCGAGAGTGACTTCGCCGAATTTTCATGTGTGTCTGGTTTCTTCTCCACTGACCCATCACATTTTTGGTTCTC
5	X	41091860	Primary Biopsy	23.7	USP9X	3'UTR	TB86B_chrX_41091860	ATCAAGACTGTGCACCCAGGCCTTACAGTCCAACCTTTTTCTGTGTCTGGCTAATATTTAAAACTAGAAAAACTATTCCTAATCAACATGGAGTGGAGAGTTTATTCACTGTCTTATCT
5	X	44919338	Primary Biopsy	8.8	KDM6A	Silent	TB86B_chrX_44919338	AACCTTCCACAAGGTAGTCTACAGAATAAAACTAAATTACTTCCTAGTATTGAGGAGGCGTGGAGCCTACCAATTCCCGCAGAGCTTACCTCCAGGCAGGGTGCCATGAACACAGCACA
5	X	44919820	Primary Biopsy	8.5	KDM6A	Intron	TB86B_chrX_44919820	TGAAAAGTATGCAGCTTGTAAAGTTTTATAATTTGAAGGAATGAATTAAGAATATATAGAACCCTATTTTTGTCTTCCTTCTGTGATTCTTAGGCATGTAAACCTCATCATCCAAATAC
5	X	44919922	Primary Biopsy	9.3	KDM6A	Intron	TB86B_chrX_44919922	CCTCATCATCCAAATACTGAACCTGTATTAGGCCTCAGTCAAACACCAATTTCACAGCAATCCTTGCCACTACACATGATTCCTTCTAGCCAAGTAGATGACCTGTCCAGTCCTGCCAA
5	X	44919947	Primary Biopsy	9.3	KDM6A	Intron	TB86B_chrX_44919947	TATTAGGCCTCAGTCAAACACCAATTTCACAGCAATCCTTGCCACTACACATGATTCCTTCTAGCCAAGTAGATGACCTGTCCAGTCCTGCCAAGAGGAAAAGAACATCTAGTCCAACA
5	X	44920018	Primary Biopsy	12.7	KDM6A	Intron	TB86B_chrX_44920018	GATGACCTGTCCAGTCCTGCCAAGAGGAAAAGAACATCTAGTCCAACAAAGGTATATGTTTTAGAGAAATAGAAAATCCCAGTCAAAAAAGAAGTTTCAGCTGCCCTGAAATTGTGCAG
5	X	44920019	Primary Biopsy	10.4	KDM6A	Intron	TB86B_chrX_44920019	ATGACCTGTCCAGTCCTGCCAAGAGGAAAAGAACATCTAGTCCAACAAAGGTATATGTTTTAGAGAAATAGAAAATCCCAGTCAAAAAAGAAGTTTCAGCTGCCCTGAAATTGTGCAGT
5	X	44922983	Primary Biopsy	9.2	KDM6A	Missense_Mutation	TB86B_chrX_44922983	TAATCATATAACAGGAAGTGGAAGTAATGGAAACGTGCCTTACCTGCAGCGAAACGCACTCACTCTACCTCATAACCGCACAAACCTGACCAGCAGCGCAGAGGAGCCGTGGAAAAACC
5	X	44970787	Primary Biopsy	8.2	KDM6A	3'UTR	TB86B_chrX_44970787	TTTGTAGCTATCTCGTAAGGCTGCTGGCTGAAAACTGTGTCTATGCAACCTTCCAAGTGCGGAGTGTCAACCAACTGGACGGGAGAGAGTACTGCTCCTACTCCAGGACTCTCACAAAG
5	X	66942742	Primary Biopsy	10.1	AR	Silent	TB86B_chrX_66942742	CTGAAAAATCAAAAATTCTTTGATGAACTTCGAATGAACTACATCAAGGAACTCGATCGTATCATTGCATGCAAAAGAAAAAATCCCACATCCTGCTCAAGACGCTTCTACCAGCTCAC
5	X	66942763	Primary Biopsy	9.3	AR	Silent	TB86B_chrX_66942763	GATGAACTTCGAATGAACTACATCAAGGAACTCGATCGTATCATTGCATGCAAAAGAAAAAATCCCACATCCTGCTCAAGACGCTTCTACCAGCTCACCAAGCTCCTGGACTCCGTGCA
5	X	66942784	Primary Biopsy	8.7	AR	Silent	TB86B_chrX_66942784	ATCAAGGAACTCGATCGTATCATTGCATGCAAAAGAAAAAATCCCACATCCTGCTCAAGACGCTTCTACCAGCTCACCAAGCTCCTGGACTCCGTGCAGCCTGTAAGCAAACGATGGAG
5	X	70346226	Primary Biopsy	7.7	MED12	Silent	TB86B_chrX_70346226	TCTCACTCCCACTGCCCTTATCAGGTCTCCCGGAATGTTCTGGAGCAGATCACGAGCTTTGCCCTTGGCATGTCATACCACTTGCCTCTGGTGCAGCATGTGCAGTTCATCTTCGACCT
5	X	70346241	Primary Biopsy	10.2	MED12	Silent	TB86B_chrX_70346241	CCTTATCAGGTCTCCCGGAATGTTCTGGAGCAGATCACGAGCTTTGCCCTTGGCATGTCATACCACTTGCCTCTGGTGCAGCATGTGCAGTTCATCTTCGACCTCATGGAATATTCACT
5	X	70346301	Primary Biopsy	10.8	MED12	Silent	TB86B_chrX_70346301	TACCACTTGCCTCTGGTGCAGCATGTGCAGTTCATCTTCGACCTCATGGAATATTCACTCAGCATCAGTGGCCTCATCGACTTTGCCATTCAGGTGGGGAAGTTGGGGAGATGAGGGTG
5	X	70357668	Primary Biopsy	8.9	MED12	Silent	TB86B_chrX_70357668	CAGCAACACACAGGCCCTGCAGGTACCATGGTGCCCCCCAGCTACTCCAGCCAGCCTTACCAGAGCACCCACCCTTCTACCAATCCTACTCTTGTAGATCCTACCCGCCACCTGCAACA
5	X	70514277	Primary Biopsy	8.5	NONO	Silent	TB86B_chrX_70514277	CTGGAAGAAGCCTTTTCTGTGTTTGGCCAGGTAGAGAGGGCTGTAGTCATTGTGGATGATCGAGGAAGGCCCTCAGGAAAAGGCATTGTTGAGTTCTCAGGGAAGCCAGCTGCTCGGAA
5	X	70514295	Primary Biopsy	8.2	NONO	Silent	TB86B_chrX_70514295	GTGTTTGGCCAGGTAGAGAGGGCTGTAGTCATTGTGGATGATCGAGGAAGGCCCTCAGGAAAAGGCATTGTTGAGTTCTCAGGGAAGCCAGCTGCTCGGAAAGCTCTGGACAGATGCAG

Supplementary Table S2: Patient-specific hybrid capture panel evaluation in negative controls

Patient	Mutation Call Source	Number of sites	total neg cntl wt count	total neg cntl mut count	Total neg ctrl depth	Min error rate (%)	Max error rate (%)	Aggregate error rate (%)	1 error in N observations
1	Primary Biopsy	28	825316	53	825369	0.0020	0.0375	0.0064	15573
2	Primary Biopsy	35	1147864	92	1147956	0.0025	0.0368	0.0080	12478
3	Primary Private	17	412565	18	412583	0.0032	0.0071	0.0044	22921
3	Primary & Met Shared	14	292340	14	292354	0.0017	0.0091	0.0048	20882
3	(Patient 3 combined)	31	704905	32	704937	0.0017	0.0091	0.0045	22029
4	Primary Biopsy	39	3521623	235	3521858	0.0008	0.0301	0.0067	14987
5	Primary Biopsy	40	1342296	64	1342360	0.0014	0.0258	0.0048	20974

Supplementary Table S3: WES statistics and mutation counts

WES Sequencing Library	Mean Depth	On-target Capture Effiency	Total Calls Passing Filters	Total Coding Calls
Pt1 Buffy Coat	120	0.75	-	-
Pt1 Primary Bx	364	0.75	256	81
Pt2 Buffy Coat	122	0.75	-	-
Pt2 Primary Bx	342	0.73	358	106
Pt3 Buffy Coat	119	0.73	-	-
Pt3 Primary Bx	302	0.74	1351	456
Pt3 Metastasis Bx	304	0.74	1735	604
Pt4 Buffy Coat	119	0.75	-	-
Pt4 Primary Bx	346	0.74	402	135
Pt5 Buffy Coat	124	0.75	-	-
Pt5 Primary Bx	313	0.73	5922	585

Supplementary Table S4: DIDA-Seq cfDNA read counts and statistical evaluation

Patient	Month	Mutation Call Source	Bam file name	Neg. Control Mut. Read Count	Neg. Control WT Read Count	Sample Mut. Read Count	Sample WT Read Count	Negative Control VAF (%)	Sample VAF (%)	Overlap p-value	Min. Required Mut. Reads (binomial test, alpha=0.9)	ng cfDNA/ml Plasma	Mutant hGE/mL Plasma	Lowest Significant VAF (%)*
1	0.0	Primary Biopsy	pt1_tp1_dida.bam	53	825316	1187	70084	0.0064	1.67	< 0.0001	7	61.1	339.3	
1	1.4	Primary Biopsy	pt1_tp2_dida.bam	53	825316	1128	127435	0.0064	0.88	< 0.0001	12	137.5	402.1	
1	3.6	Primary Biopsy	pt1_tp3_dida.bam	53	825316	1135	130097	0.0064	0.86	< 0.0001	12	130.8	377.2	
1	5.0	Primary Biopsy	pt1_tp4_dida.bam	53	825316	1374	118034	0.0064	1.15	< 0.0001	11	24.0	92.1	
1	6.9	Primary Biopsy	pt1_tp5_dida.bam	53	825316	1088	97684	0.0064	1.10	< 0.0001	10	12.4	45.5	
1	14.3	Primary Biopsy	pt1_tp6_dida.bam	53	825316	1375	111417	0.0064	1.22	< 0.0001	11	11.1	45.3	
2	0.0	Primary Biopsy	pt2_tp1_dida.bam	92	1147864	9	201752	0.0080	0.005	0.007	21	47.5	0.7	
2	0.5	Primary Biopsy	pt2_tp2_dida.bam	92	1147864	4	162942	0.0080	0.003	0.17	18	61.2	0.5	
2	4.2	Primary Biopsy	pt2_tp3_dida.bam	92	1147864	9	173283	0.0080	0.005	0.18	19	15.1	0.3	
2	10.7	Primary Biopsy	pt2_tp4_dida.bam	92	1147864	23	184383	0.0080	0.013	0.005	20	14.8	0.6	0.013
2	13.5	Primary Biopsy	pt2_tp5_dida.bam	92	1147864	21	21006	0.0080	0.100	< 0.0001	3	5.8	1.9	
2	15.6	Primary Biopsy	pt2_tp6_dida.bam	92	1147864	10	213458	0.0080	0.005	0.068	22	14.6	0.2	
2	18.0	Primary Biopsy	pt2_tp7_dida.bam	92	1147864	20	279028	0.0080	0.007	0.1757	28	12.7	0.3	
3	0.0	Primary Private	pt3_tp1_dida.bam	18	412565	30	90514	0.0044	0.033	< 0.0001	7	8.8	96.7	
3	1.8	Primary Private	pt3_tp2_dida.bam	18	412565	27	121504	0.0044	0.022	0.0001	8	32.4	240.0	
3	3.5	Primary Private	pt3_tp3_dida.bam	18	412565	111	127103	0.0044	0.087	< 0.0001	9	24.4	709.8	
3	4.2	Primary Private	pt3_tp4_dida.bam	18	412565	3	144844	0.0044	0.002	0.22	10	24.4	17.1	
3	10.1	Primary Private	pt3_tp5_dida.bam	18	412565	31	96929	0.0044	0.032	< 0.0001	7	12.4	131.9	0.032
3	0.0	Primary & Met Shared	pt3_tp1_dida.bam	14	292340	160	62213	0.0048	0.257	< 0.0001	5	8.8	749.6	
3	1.8	Primary & Met Shared	pt3_tp2_dida.bam	14	292340	125	81831	0.0048	0.153	< 0.0001	7	32.4	1648.5	
3	3.5	Primary & Met Shared	pt3_tp3_dida.bam	14	292340	1412	86893	0.0048	1.599	< 0.0001	7	24.4	13001.4	
3	4.2	Primary & Met Shared	pt3_tp4_dida.bam	14	292340	3	101515	0.0048	0.003	0.27	8	5.2	5.2	
3	10.1	Primary & Met Shared	pt3_tp5_dida.bam	14	292340	216	66731	0.0048	0.323	< 0.0001	6	12.4	1329.5	
4	0.0	Primary Biopsy	pt4_tp1_dida.bam	235	3521623	172	160456	0.0067	0.107	< 0.0001	15	3	115.5	
4	0.4	Primary Biopsy	pt4_tp2_dida.bam	235	3521623	494	203600	0.0067	0.242	< 0.0001	18	8	677.6	
4	1.4	Primary Biopsy	pt4_tp3_dida.bam	235	3521623	29	266181	0.0067	0.011	0.047	23	160	582.5	0.011
4	4.6	Primary Biopsy	pt4_tp4_dida.bam	235	3521623	5	114164	0.0067	0.004	0.1055	11	7	10.4	
4	4.6	Primary Biopsy	pt4_tp5_dida.bam	235	3521623	29	134977	0.0067	0.022	< 0.0001	13	0	1.6	
4	6.1	Primary Biopsy	pt4_tp6_dida.bam	235	3521623	5	208223	0.0067	0.002	0.01	19	11	9.2	
5	0.0	Primary Biopsy	pt5_tp1_dida.bam	65	1358753	54	405053	0.0048	0.0133	0.0001	25	74.0	328.1	
5	1.3	Primary Biopsy	pt5_tp2_dida.bam	65	1358753	13	164500	0.0048	0.0079	0.16	12	19.0	50.1	0.0079
5	3.0	Primary Biopsy	pt5_tp3_dida.bam	65	1358753	5	180035	0.0048	0.0028	0.16	12	37.7	35.2	
5	4.9	Primary Biopsy	pt5_tp4_dida.bam	65	1358753	8	177422	0.0048	0.0045	0.066	12	26.6	39.9	
5	5.1	Primary Biopsy	pt5_tp5_dida.bam	65	1358753	5	215050	0.0048	0.0023	0.10	15	50.5	38.7	
5	7.4	Primary Biopsy	pt5_tp6_dida.bam	65	1358753	1	206177	0.0048	0.0005	0.002	14	12.2	2.0	